C.P. No. 313
(18,872)
A.R.C. Technical Report

C.P. No. 313
(18,872)
A.R.C. Technical Report

MINISTRY OF SUPPLY

AERONAUTICAL RESEARCH COUNCIL

CURRENT PAPERS

Charts of the Theoretical Wave Drag of Wings at Zero-Lift

By

R. A. Bishop, and E. G. Cane

LONDON: HER MAJESTY'S STATIONERY OFFICE

1957

FIVE SHILLINGS NET

C.P. No.313

U.D.C. No. 533.6.013.12:533.691.11

Technical Note No. Aero 2421

June, 1956

ROYAL AIRCRAFT ESTABLISHMENT

Charts of the theoretical wave drag of wings at zero-lift

by

R. A. Bishop
and
E. G. Cane

SUMMARY

Charts are presented for the theoretical wave drag at zero-lift of straight-tapered wings with streamwise tips, and with double-wedge or parabolic-arc sections. A bibliography of theoretical reports is included, and their contents are reviewed.

This note supersedes R.A.E. Technical Note No. Aero 2139 revised (CP 116), which contains errors.

LIST OF CONTENTS

LIST OF ILLUSTRATIONS

1 Introduction

This note has been written to supersede RAE Tech. Note No. Aero 2319 revised (CP 116)[1], and to give a new standard set of charts of linear theory wave drag at zero lift, since certain errors were found after the previous note had been issued. A complete revision has been made, and, whilst we have followed the methods of analysis and presentation adopted by Lawrence, the opportunity has been taken to extend the scope of the work by including more recent results.

As in Lawrence's report, the wings considered all have straight leading and trailing edges, streamwise tips and a constant thickness-chord ratio. The new results introduced include the values given by linear theory for the drag when $A\sqrt{M^2 - 1} = 0$ for all the wings considered, and also the available results for fully tapered wings of parabolic-arc section. There is still a lack of results for wings of parabolic-arc section and arbitrary taper, and for wings of arbitrary section and general planform.

It is worth emphasising that this note is concerned with theoretical results only: work is actively proceeding on comparisons between theory and experiment.

2 Presentation of results

2.1 Choice of parameters

Three geometrical parameters are required to define a wing planform with straight edges and streamwise tips (see Fig.1(a)), and we have chosen the aspect ratio A, the sweepback of the half-chord line $\Lambda_{\frac{1}{2}}$ and the taper ratio λ.

The supersonic similarity laws show that for wings of similar section,

$$\frac{C_D}{A\tau^2} = f\left(A\sqrt{M^2 - 1},\ A \tan \Lambda_{\frac{1}{2}},\ \lambda\right)$$

where C_D = wave drag coefficient; τ = thickness/chord ratio.

We have therefore adopted the similarity parameters given in this equation in the presentation. This selection of parameters has been found to be the most illuminating and follows that used by Stanbrook[2] for the lifting properties of wings.

We have chosen a range of values of λ of 0, 0.2, 0.5 and 1. The parameter $\frac{(1-\lambda)}{(1+\lambda)}$ then has values of 1, $^2/_3$, $^1/_3$ and 0, and since the curves are nearly linearly spaced with respect to $\frac{(1-\lambda)}{(1+\lambda)}$, linear interpolation for other taper ratios is reasonably accurate.

2.2 Shape of drag curves

Due to the approximations of linear theory, kinks occur in the drag curves when lines across which the flow is turned through a finite angle become sonic, namely leading and trailing edges and ridge-lines of polygonal sections. These kinks are not realised in practice since they correspond to flow conditions for which the linearised equation is no longer valid.

In addition to these kinks, there are finite changes in the curvature of the drag curves whenever a Mach line from one of the discontinuities in slope of the root section (leading edge, trailing edge or ridge-line), crosses a discontinuity in slope of the tip section. Similar changes occur when there is interaction between the tips. In general these changes are small, and they are shown in the curves only for untapered wings, where several interactions are superimposed to produce rather larger changes in curvature.

In Fig.1(b) the general cases are shown for which kinks and changes in curvature occur. The corresponding values of the Mach number can be obtained from the following formulae. When there is interaction between centre-line chord and the tip, then

$$A\sqrt{M^2 - 1} = \left| A \tan \Lambda_{\frac{1}{2}} + \frac{2(1 - 2h - \lambda [\, 1 - 2h_t])}{1 + \lambda} \right| \qquad (1)$$

and when the tips interact,

$$A\sqrt{M^2 - 1} = \left| \frac{2\lambda\left(h_{t_1} - h_{t_2}\right)}{1 + \lambda} \right| \qquad (2)$$

where h is a fraction of the centre-line chord aft of the wing apex; and h_t, h_{t_1} and h_{t_2} are all fractions of the tip chord aft of the leading edge of the tip.

3 Source of data

3.1 Double-wedge sections

3.11 Fully tapered planforms

Some of the early results for tapered wings were due to Puckett[4], who considered the drag of the delta wing, of true triangular planform, for various maximum thickness positions. Later in reference 5 he extended his calculations to particular sweptback wings. These were for values of $A \tan \Lambda_{\frac{1}{2}} = 2$ (the delta wing) and $A \tan \Lambda_{\frac{1}{2}} = 6$, for a consistent range of maximum thickness positions, and for subsonic and supersonic leading edges.

The results of Multhopp and Winter[6] have been used to derive the bulk of Figs.2(a), 2(b), 2(c), 2(d) and 2(e). These authors have prepared charts from which the drag of fully tapered wings with double-wedge sections can be easily computed. In addition, these results can be applied to wings with polygonal sections, but the calculations become very laborious.

Between the above references, and also references 7, 9, and 10 there is some overlap in the results, but they are all in agreement within the accuracy of the calculations.

3.12 Planforms of arbitrary taper

The curves for the unswept wings ($A \tan \Lambda_{\frac{1}{2}} = 0$), have been derived from Nielsen[7], who has evaluated this case for a range of λ of 0, 0.25, 0.5, 0.75 and 1, but only for maximum thickness position at half-chord ($m = 0.5$). The remainder of Figs.3 and 4(a) has been prepared using the work of Chang[8], who presents charts for the particular values of λ of 0.2 and 0.5. Chang's

results have only been used for large values of $A\sqrt{M^2 - 1}$, as the data cannot be crossplotted with sufficient accuracy at lower values. Margolis's[9,10] equations have been computed to provide the results for the lower range, and have also been evaluated at the higher values of $A\sqrt{M^2 - 1}$ to verify Chang's results.

3.13 Untapered planforms

This case has been dealt with fully by Margolis[11], who gives equations for arbitrary maximum thickness position. Two values of m, the maximum thickness position as a fraction of the chord, have been chosen, m = 0.3 and 0.5, and the results are presented in Figs.5(a) and 5(b). Since the equations for the drag are symmetrical with respect to the maximum thickness position, the results for m = 0.3 cover also the case m = 0.7. For $A\sqrt{M^2 - 1} > A \tan \Lambda_{\frac{1}{2}} + 2$ the drag coefficient for the swept untapered wing is the same as that of an infinite swept wing namely,

$$\frac{C_D}{A\tau^2} = \frac{1}{\sqrt{A^2 (M^2 - 1) - A^2 \tan^2 \Lambda_{\frac{1}{2}}}} \cdot \frac{1}{m (1 - m)}$$

This formula shows how the drag coefficient varies with maximum thickness position, and helps in the interpolation between the curves.

For $A\sqrt{M^2 - 1} > 1$ the rectangular wing ($A \tan \Lambda_{\frac{1}{2}} = 0$) has the same drag as the two-dimensional wing i.e. $\frac{C_D}{A\tau^2} = \frac{1}{A\sqrt{M^2 - 1}} \cdot \frac{1}{m(1 - m)}$

For $A\sqrt{M^2 - 1} < 1$ the curve for the rectangular wing with m = 0.5 has been obtained from Nielsen[7].

3.2 Parabolic-arc sections

3.21 Tapered planforms

The work of Beane[12] and Picard[13] has been presented in Figs. 2(f) and 4(b). For fully tapered wings Beane has given results for values of $A \tan \Lambda_{\frac{1}{2}} = 0$, 2 and 2.8, whilst Picard has worked out the drag when $A \tan \Lambda_{\frac{1}{2}} = 2$, 3, and 4.6. For the common value of $A \tan \Lambda_{\frac{1}{2}} = 2$ the results are in excellent agreement.

Beane also presents charts for values of λ of 0.25 and 0.50, and values of $A \tan \Lambda_{\frac{1}{2}}$ between 0 and 2.8. The data is only given for supersonic leading edges, and the size of the charts does not permit accurate crossplotting. However we have decided to present the data for $\lambda = 0.5$ in Fig.4(b) in order to give some idea of the effect of taper ratio.

3.22 Untapered planforms

Fig.5(c) has been derived from references 14 and 15. The drag can be obtained from the charts given in the two reports, but not sufficiently accurately for presentation, and so the curves shown here have been recomputed from the original formulae.

3.3 Wave drag when $A\sqrt{M^2 - 1} = 0$

Although the values given by linear theory for the wave drag when $A\sqrt{M^2 - 1} = 0$ sometimes appear unrealistic, they have been included for completeness and because, without much difficulty in computing, they offer a guide in determining the shape of the drag curves in this region. The significance of the value of the wave-drag given by linear theory must be interpreted individually for each wing. For instance, for a wing which has a nearly constant drag coefficient near $A\sqrt{M^2 - 1} = 0$, the result can be used as a measure of the transonic drag rise. For other wings the meaning of the value must be carefully assessed. The predicted drag may, for example, be unduly high because the trailing edge has only a small angle of sweep, but the result may still be of use in comparing one wing with another having similar trailing edge conditions.

Some curves near $A\sqrt{M^2 - 1} = 0$ have been shown as dashed lines to indicate that over this range the curves have not been verified by calculations.

3.31 Double-wedge sections

Puckett and Stewart[5] have found a solution for the wave drag of fully tapered wings for $A\sqrt{M^2 - 1} = 0$. This has been used to give the end points for Fig.2. The results for the tapered and untapered wings are due to Cane[17], and have been evaluated using the area rule.

3.32 Parabolic-arc sections

The results for fully tapered wings have been computed from a formula given by Nonweiler[16], except for $A \tan \Lambda_{\frac{1}{2}} = 0$. This curve and the results for $\lambda = 0.5$ have been calculated numerically using the area rule method given in reference 18. For the untapered wings we have used the explicit formula given by Harmon and Swanson[14], which has recently been verified by Lord, Ross and Eminton[18].

4 Discussions

4.1 Effect of maximum thickness position

4.11 Double-wedge sections

The effect of maximum thickness position on the wave drag of wings with double-wedge sections is shown in Fig.6 for $\lambda = 0$ and in Fig.7 for $\lambda = 1$.

Puckett[4] shows that for fully tapered wings, the optimum position of the maximum thickness is approximately at 20% of the chord if the leading edge is subsonic, and between 50% and 60% of the chord if the leading edge is supersonic. It is seen from Fig.6 that the increment in drag due to changing the maximum thickness position is roughly constant over the range of values of $A\sqrt{M^2 - 1}$, provided the lines of maximum thickness of the wings being compared are either both subsonic or both supersonic.

In the case of untapered wings, the theory predicts that for subsonic edges the position of maximum thickness has little effect. But for supersonic edges, Margolis's results show that there is a well-defined optimum with maximum thickness position at the half-chord.

4.12 Parabolic-arc sections

Beane has considered the effect of maximum thickness position on the drag of wings of parabolic-arc section, but only for a particular sweptback fully tapered wing. However in this case the optimum positions of maximum thickness are roughly the same as those for wings of double-wedge section, and Sheppard[29] has shown that this is also true for untapered wings.

4.2 Effect of taper

Fig.8 shows the effect of taper on the wave drag, for values of $A \tan \Lambda_{\frac{1}{2}} = 0$, 1, 2 and 4, for wings having symmetrical double-wedge sections ($m = 0.5$). It is apparent that taper has an important effect for subsonic trailing edges, especially near $A\sqrt{M^2 - 1} = 0$, whilst for supersonic leading edges the effect is not nearly so noticeable, since the drag coefficient is tending to the two-dimensional value.

There is not sufficient information to show, in detail, the effect of taper for wings having parabolic-arc sections, but, from the two cases which we have shown in Fig.8, the general conclusions given for the double-wedge sections also appear to be true here.

LIST OF SYMBOLS

A	Aspect ratio
b	span
c_o	centre line chord
c_t	tip chord
C_D	wave drag coefficient
f	arbitrary function
h	a fraction of the centre-line chord aft of the wing apex
h_t, h_{t_1}, h_{t_2}	fraction of the tip chord aft of the leading edge of the tip
M	Mach number
m	maximum thickness position as a fraction of the chord
$\Lambda_{\frac{1}{2}}$	sweepback of half-chord line
λ	taper ratio, ratio of tip chord to root chord
μ	Mach angle $= \operatorname{cosec}^{-1} M$
τ	thickness/chord ratio

REFERENCES

No.	Author	Title etc.
1	T.F.C. Lawrence	Charts of the wave drag of wings at zero-lift. RAE Tech. Note No.2139 (Revised) ARC 15,595 (CP 116) November, 1952.
2	A. Stanbrook	Lift-curve slope at subsonic and supersonic speeds. Aircraft Engineering, Vol.XXVI No. 306, pp 244-246. August, 1954.
3	R.T. Jones	Thin oblique aerofoils at supersonic speeds. NACA TN 1107 September, 1946.
4	A.E. Puckett	Supersonic wave drag of thin airfoils. Journal Aeronautical Sciences 1946 Vol.13 No.9 pp 475-485.
5	A.E. Puckett and H.J. Stewart	Aerodynamic performance of delta wings at supersonic speeds. Journal Aeronautical Sciences 1947 Vol.14, No.14 pp 567-578.
6	H. Multhopp and M. Winter	Charts for the calculation of the wave drag of swept wings. RAE Unpublished.
7	J.N. Nielsen	The effect of aspect ratio and taper on the pressure drag at supersonic speeds of unswept wings at zero-lift. NACA Tech. Note 1487 November, 1947.
8	C.C. Chang	Applications of Von Karman's Integral method in supersonic wing theory. NACA Tech Note 2317 March, 1951.
9	K. Margolis	Supersonic wave drag of sweptback tapered wings at zero lift. NACA Tech Note 1448 October, 1947 (TIB/1189).
10	K. Margolis	Supersonic wave drag of non-lifting sweptback tapered wings with Mach lines behind the line of maximum thickness. NACA Tech Note 1672 August, 1948.
11	K. Margolis	Effect of chordwise location of maximum thickness on the supersonic wave drag of sweptback wings. NACA Tech Note 1543 March, 1948.
12	B. Beane	The characteristics of supersonic wings having biconvex sections. Journal Aeronautical Sciences 1951 Vol.18 No.1 pp 7-20.

REFERENCES (Contd.)

No.	Author	Title etc.
13	C. Picard	Caractéristiques aérodynamiques théoriques des ailes delta et des ailes en queue d'hirondelle. La Recherche Aéronautique Mai-Juin, 1954 Numéro 39 pp 15-26.
14	S. Harmon and M. Swanson	Calculations of the supersonic wave drag of non-lifting wings with arbitrary sweepback and aspect ratio - wings swept behind the Mach lines. NACA Tech Note 1319 May, 1947 (TIB/1117).
15	S. Harmon	Theoretical supersonic wave drag of untapered sweptback and rectangular wings at zero lift. NACA Tech Note 1449 October, 1947.
16	T. Nonweiler	The theoretical wave drag at zero lift of fully tapered swept wings of arbitrary section. College of Aeronautics Report No.76 ARC 16,531 October, 1953.
17	E.G. Cane	Theoretical wave drag of wings of double-wedge section at M = 1. RAE Note to be published.
18	W.T. Lord, A.J. Ross and E. Eminton	Theoretical drag rise of wings at transonic speeds. RAE Tech Note No. Aero 2267 ARC 16785 April, 1954
19	A. Ferri	Elements of aerodynamics of supersonic flow. The MacMillan Company: New York, 1949
20	E.A. Bonney	Aerodynamic characteristics of rectangular wings at supersonic speeds. Journal Aeronautical Sciences 1947 Vol.14 No.2 pp 110-116.
21	E.A. Eichelbrenner	Trainée d'onde des ailes en flèches à profils losangiques aux vitesses supersoniques. La Recherche Aéronautique Nov-Dec. 1949.
22	E.A. Eichelbrenner	Trainée d'onde des ailes en flèches effilées à profils losangiques aux vitesses supersoniques. La Recherche Aéronautique Sept-Oct 1950.
23	A. Robinson	The wave drag of diamond-shaped aerofoils at zero incidence. RAE Tech Note No. Aero 1784 May, 1946 ARC 9780 R & M 2394.

REFERENCES (Contd.)

No.	Author	Title etc.
24	A. Robinson	Wave drag of an aerofoil at zero incidence. RAE Report No. Aero 2159 September, 1946 ARC 10311.
25	J. Kleissas	Charts of the zero-lift drag of supersonic sweptback wings for various taper ratios. Northrop Report GM 109 September, 1947
26	O.K. Smith	Applications of the Von Karman Theory of Linearised Supersonic Flow. Northrop Report No. GM 106 Parts II & III.
27	D.C.M. Leslie and J.D. Perry	Wave drag of wings at supersonic speeds. Proceedings Royal Society 1954 Vol.225 pp 213-225.
28	F.C. Grant and M. Cooper	Tables for the computation of wave drag of arrow wings of arbitrary airfoil section. NACA Tech Note 3185 June, 1954
29	L.M. Sheppard	A method for determining the maximum thickness position for minimum wave drag of wings with supersonic edges. HSA TN 12 September, 1954
30	M. Bismut	Détermination rapide des traînées d'onde d'ailes en queue d'hirondelle. La Recherche Aéronautique 1951 No.21.
31	E. Lapin	Charts for the computation of lift and drag of finite wings at supersonic speeds. Douglas Report No. SM-13480 October, 1949.
32	J.H. Kainer	Theoretical calculations of the supersonic pressure distribution and wave drag for a limited family of tapered sweptback wings with symmetrical parabolic-arc sections at zero lift. NACA TN 2009 January, 1950.
33	M.M. Shaw	Analysis of theoretical results on the effect of section and taper on wing wave drag. RAE Unpublished.
34	T. Nonweiler	Theoretical supersonic drag of non-lifting infinite span wings swept behind the Mach lines. RAE Tech Note No. Aero 2073 October, 1950 ARC 13,896 R & M 2795.

APPENDIX

Bibliography of theoretical data

A list is given of theoretical reports on wave drag, with notes outlining the scope of the work covered and the results presented in the reports. It is not intended to provide a comprehensive list of references, but to summarise the various works relevant to this note.

Author	Ref.	Notes
Jones	3	Thin aerofoil theory is applied to calculate the pressure distribution over swept wings of symmetrical double-wedge and parabolic-arc sections. The pressure distribution over an untapered swept wing of parabolic-arc section is plotted, and indication given as to the method of solution for tapered wings.
Puckett	4	The author uses source distribution methods to compute the wave drag of a delta wing of double-wedge section, for subsonic and supersonic leading-edges. The effect of maximum thickness position is considered.
Puckett, Stewart	5	The work of reference 4 is extended, and equations for fully tapered wings are derived for various maximum thickness positions. Charts are presented giving the drag of a delta wing ($A \tan \Lambda_{\frac{1}{2}} = 2$) and a general swept wing ($A \tan \Lambda_{\frac{1}{2}} = 6$), for $m = 0.2$ to 0.5. A formula for the drag at $M = 1$ is given.
Multhopp Winter	6	Functions are given from which the drag of fully tapered wings of double-wedge section can be evaluated. Modified wedge sections can be considered, but the computations become laborious.
Nielsen	7	Expressions are derived for the drag of unswept wings of double-wedge section, $m = 0.5$ and arbitrary taper. Equations are presented for $0 < \lambda < 1$, and simplified equations for $\lambda = 0$ and $\lambda = 1$. The results are given in charts from which the drag can be deduced for $\lambda = 0, \frac{1}{4}, \frac{1}{2}, \frac{3}{4}$ and 1.
Chang	8	Von Karman's Fourier Integral method is used to calculate the wave drag of sweptback wings of symmetrical double wedge section for both intermediate and full taper. The formula given for the drag at $M = 1$ is incorrect. The results of calculations for $\lambda = 0.2$ and $\lambda = 0.5$ are presented in charts, and the drag can be directly read.

APPENDIX (Contd.)

Author	Ref.	Notes
Margolis	9	Equations are derived for the drag of tapered wings of symmetrical double-wedge section for $0 < \lambda < 1$, for subsonic maximum thickness line. The limiting solutions are also given for $\lambda = 0$ and $\lambda = 1$.
Margolis	10	The work of reference 9 is extended to wings with supersonic maximum thickness line.
Margolis	11	Equations showing the effect of maximum thickness position on the drag of untapered wings of double-wedge section are derived, and it is found that the optimum position is at the half-chord, if the tip does not affect the other half of the wing.
Eichelbrenner	21	Source distribution methods are used to calculate the wave drag of untapered wings of symmetrical double-wedge section with maximum thickness at the half-chord. The analysis is not explained in detail.
Eichelbrenner	22	The work of reference 21 is extended to include the wave drag of tapered wings, and the results are presented in charts. The results are not compared with Margolis, and it has been found that the results of this work are not correct.
Robinson	23	The pressure distribution and wave drag is calculated of a wing of double-wedge section and symmetrical diamond planform. The drag is compared with that obtained by strip theory, but the plotted results are in error for $\tan\gamma/\tan\mu < 1$. (γ = leading-edge sweep).
Robinson	24	The calculations made in ref.23 are described in detail.
Kleissas	25	The author computes the drag of tapered wings of symmetrical double-wedge section for subsonic leading edges from formulae given in an earlier report by Smith[26]. The results are presented in charts for various values of λ, but are not in agreement with the results of Margolis or Chang, and it is thought that this is because the author has used numerical methods of integration.
Grant, Cooper	28	Tables are given from which the drag can be computed for fully tapered wings of arbitrary section. The wing section is replaced by twenty equally spaced straight segments and the drag is evaluated using source distributions. A range of $A \tan \Lambda_{\frac{1}{2}} \sqrt{M^2 - 1}$ cot Λ_o from 0 to 18 is covered, and from 0.2 to 4.

APPENDIX (Contd.)

Author	Ref.	Notes
Ferri	19	A detailed discussion is given on the use of source distribution methods to calculate the wave drag. The author considers the infinite yawed and infinite triangular wings, and double-wedge and parabolic-arc sections. He presents some of Pucketts results for fully tapered wings of double-wedge section, and independently derives the wave drag of a family of fully tapered wings for A tan $\Lambda_{\frac{1}{2}} < 2$, and various maximum thickness positions.
Beane	12	Source distribution methods are used to calculate the wave drag of tapered wings of parabolic-arc section. The profile is replaced by a polygon with sixteen sides. Charts are presented from which the drag can be read for $\lambda = 0$, $\frac{1}{4}$ and $\frac{1}{2}$, for low values of A tan $\Lambda_{\frac{1}{2}}$ and supersonic leading-edges. The scale of the charts prevents accurate cross-plotting.
Picard	13	The method based on a polygonal approximation, suggested by Bismut in reference 30, is used to calculate the drag of fully tapered wings of parabolic-arc section. Charts giving the drag for three values of A tan $\Lambda_{\frac{1}{2}} = 2,3$ and 4.6 are presented. The results for the delta wing are in agreement with Beane.
Harmon, Swanson	14	The method suggested by Jones in reference 3 is used to calculate the drag of untapered wings of parabolic-arc section. Equations are derived for the drag for subsonic leading edges, and also for the limiting case of $M = 1$. The authors give the results in charts, but do not allow accurate reading.
Harmon	15	The author extends the results of reference 14 to wings with supersonic leading-edges.
Kainer	32	Numerical methods are used to evaluate the drag of a particular wing of parabolic-arc section, A tan $\Lambda_{\frac{1}{2}} = 2.77, \lambda = 0.53$ and $A\sqrt{M^2 - 1} = 4.65$.
Nonweiler	16	An expression is obtained for the wave drag of fully tapered wings of arbitrary section, in the form of a double integral. The author suggests that in general the drag will need to be computed by numerical integration, but a direct integration is obtained to give a formula for the drag of wings of various sections, including a parabolic-arc section near $A\sqrt{M^2 - 1} = 0$.

APPENDIX (Contd.)

Author	Ref.	Notes
Lapin	31	The wave drag of wings of polygonal section is evaluated, provided the edges are swept, using superimposed source distributions. The individual contributions of each facet of the wing are given in charts and have to be combined to give the total drag of the wing. Subsonic and supersonic edges are considered, and results can be obtained for $A\sqrt{M^2 - 1} = 0$.
Bonney	20	Busemann's second order approximation is applied to a double-wedge section. The results are extended to other sections, including parabolic-arc sections.
Shaw	32	The drag is computed of untapered wings of symmetrical double-wedge and parabolic-arc sections using references 11, 14 and 15. It is shown that for supersonic edges, the ratio of the drags of these wings is approximately equal to the ratio of the drags of their sections.
Nonweiler	33	The author investigates the drag of untapered swept wings of infinite span, with subsonic edges and arbitrary section. The drags of a number of sections are compared with that for the parabolic-arc section, and a correction factor is derived, which it is suggested may be applied to the results for wings of parabolic-arc section, with subsonic edges and of high aspect ratio.
Leslie, Perry	27	For wings with supersonic leading-edges, the drag is found by correcting the results obtained from strip theory. The method is applied to double-wedge wings with bevelled tips.

WT.2078.CP.313.K3. Printed in Great Britain.

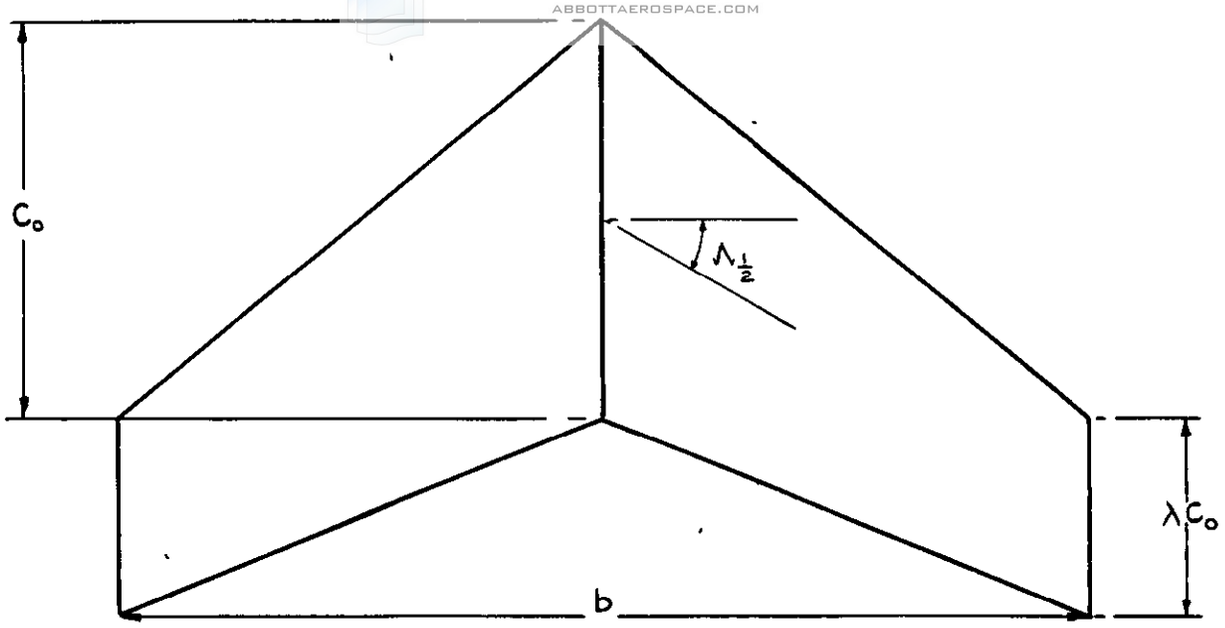

FIG. 1 (a). WING NOTATION.

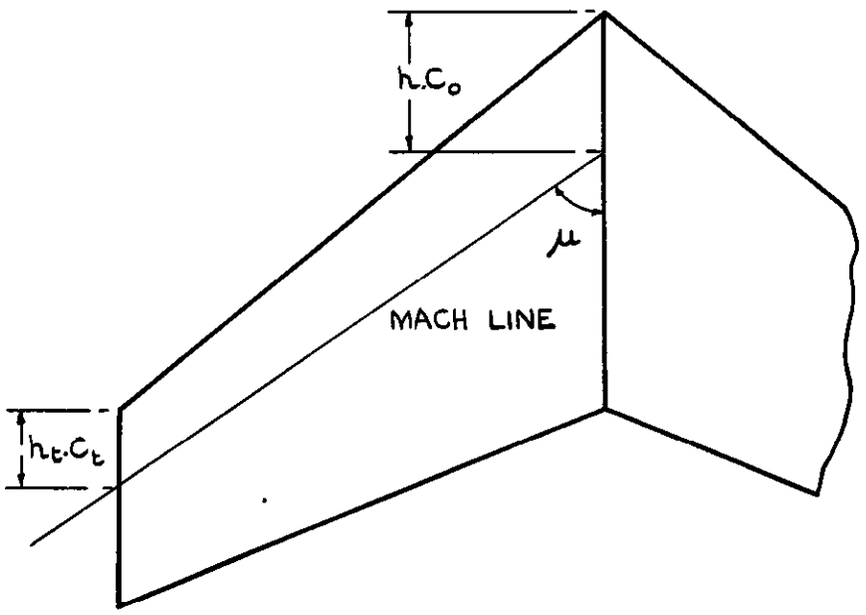

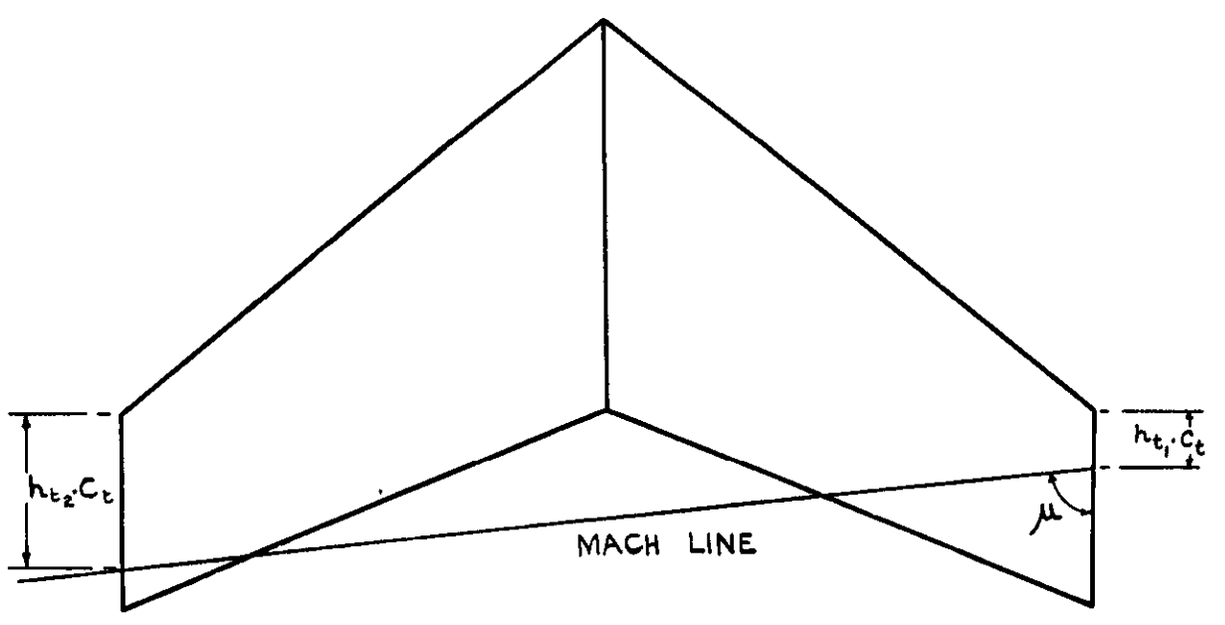

FIG. 1 (b). MACH LINE CONFIGURATIONS.

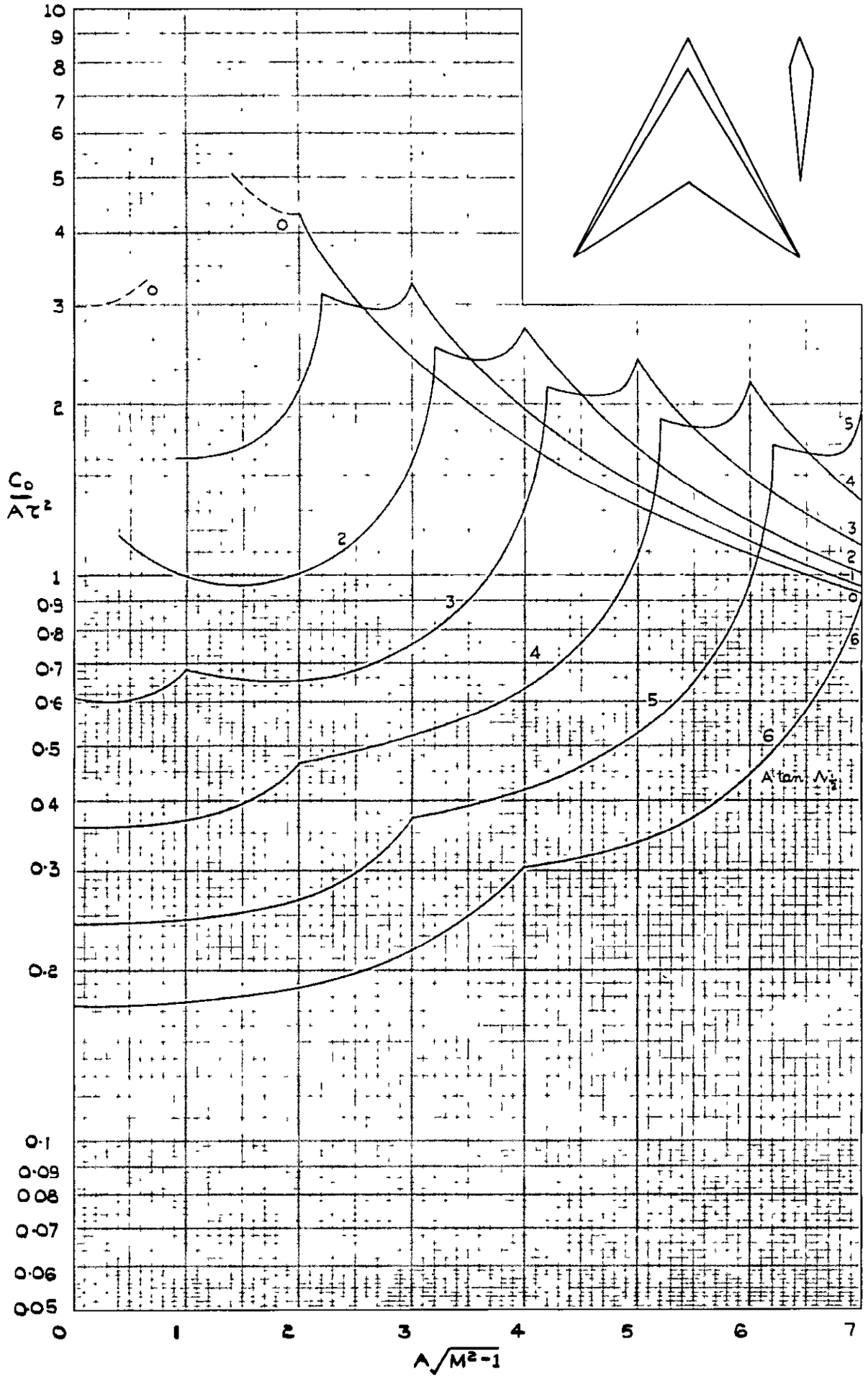

FIG. 2 (a). WAVE DRAG OF WINGS OF DOUBLE-WEDGE SECTION $\lambda = 0$, $m = 0{\cdot}2$.

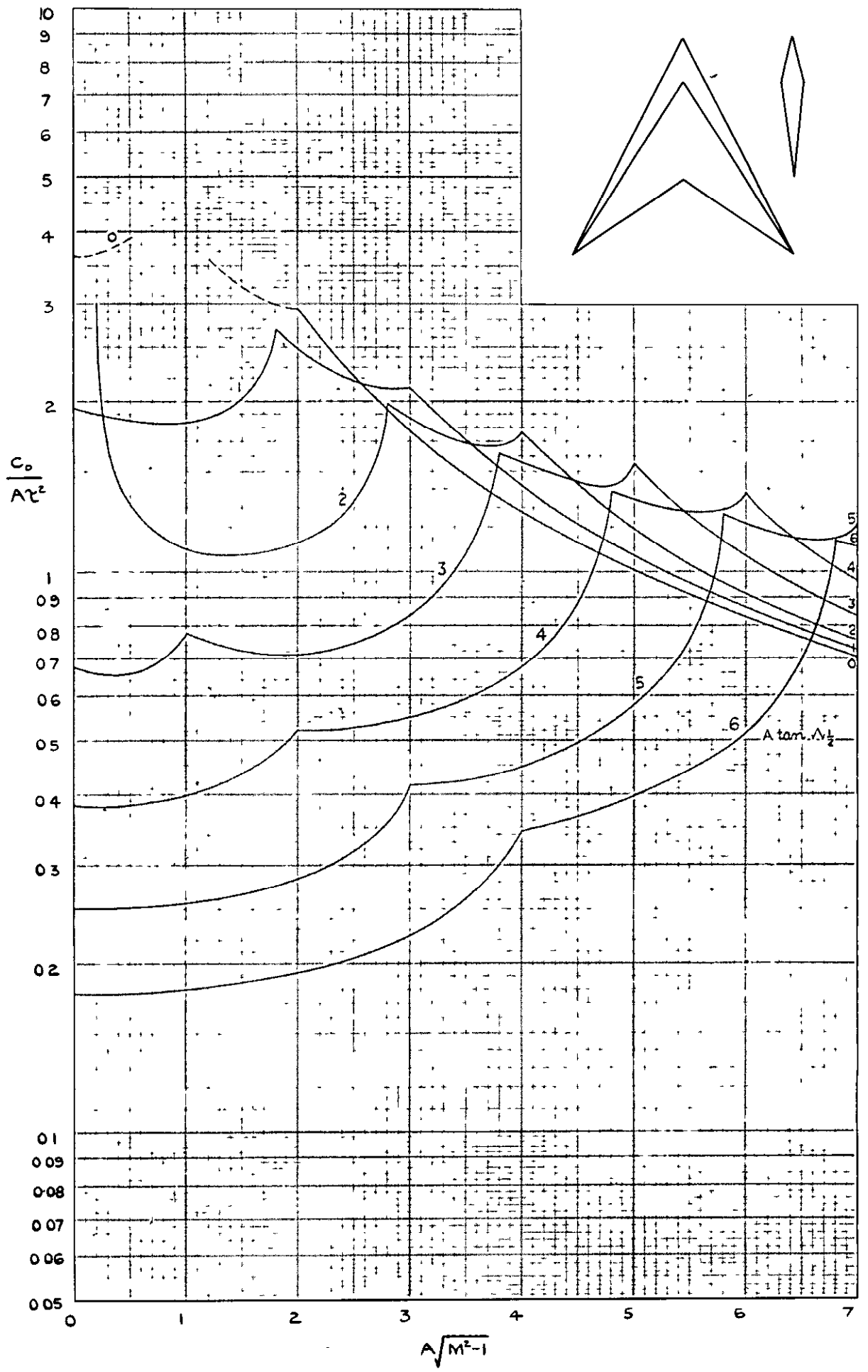

FIG. 2 (b). WAVE DRAG OF WINGS OF DOUBLE - WEDGE SECTION.

$\lambda = 0$, $m = 0{\cdot}3$

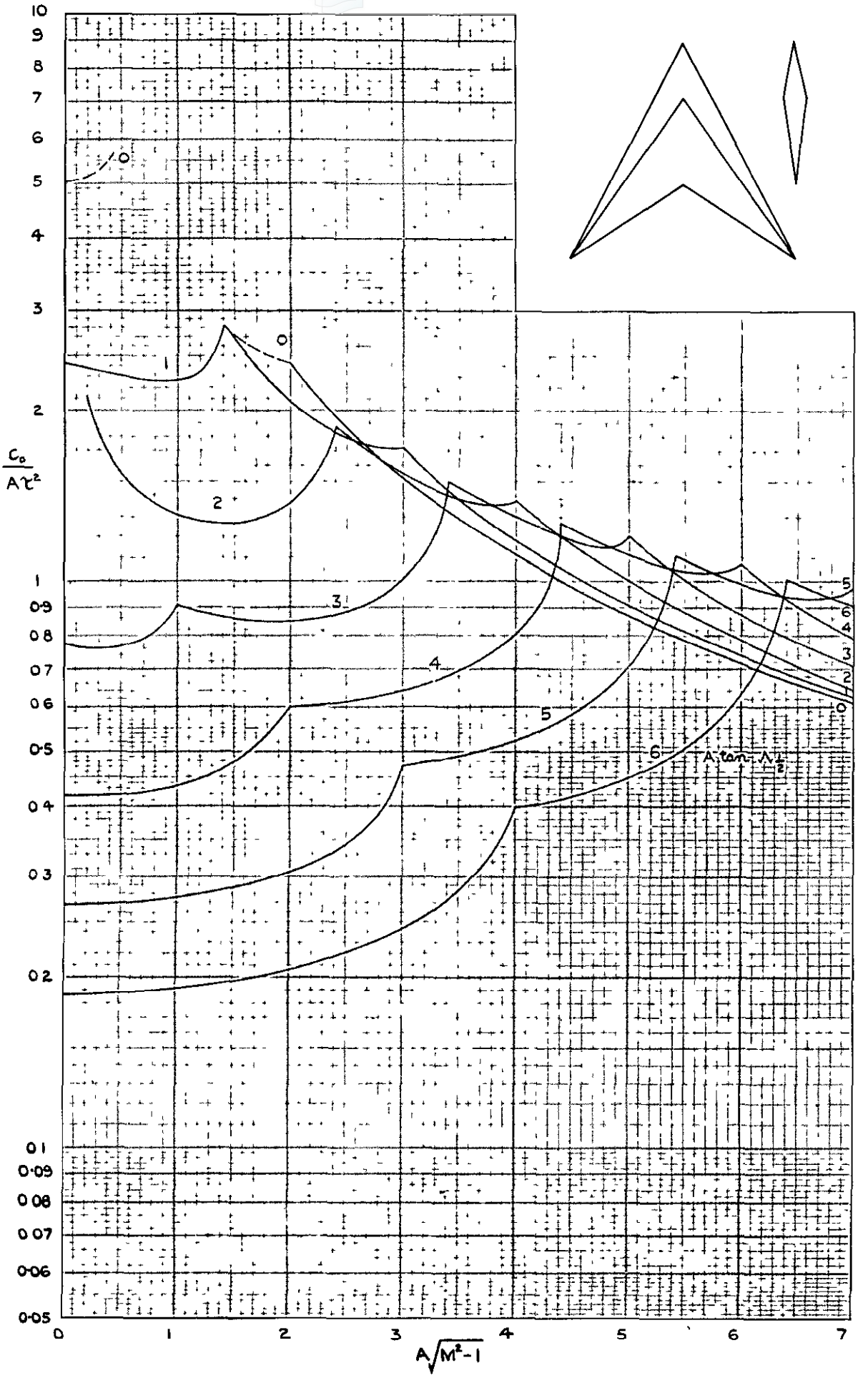

FIG. 2 (c). WAVE DRAG OF WINGS OF DOUBLE - WEDGE SECTION.
$\lambda = 0$, $m = 0.4$

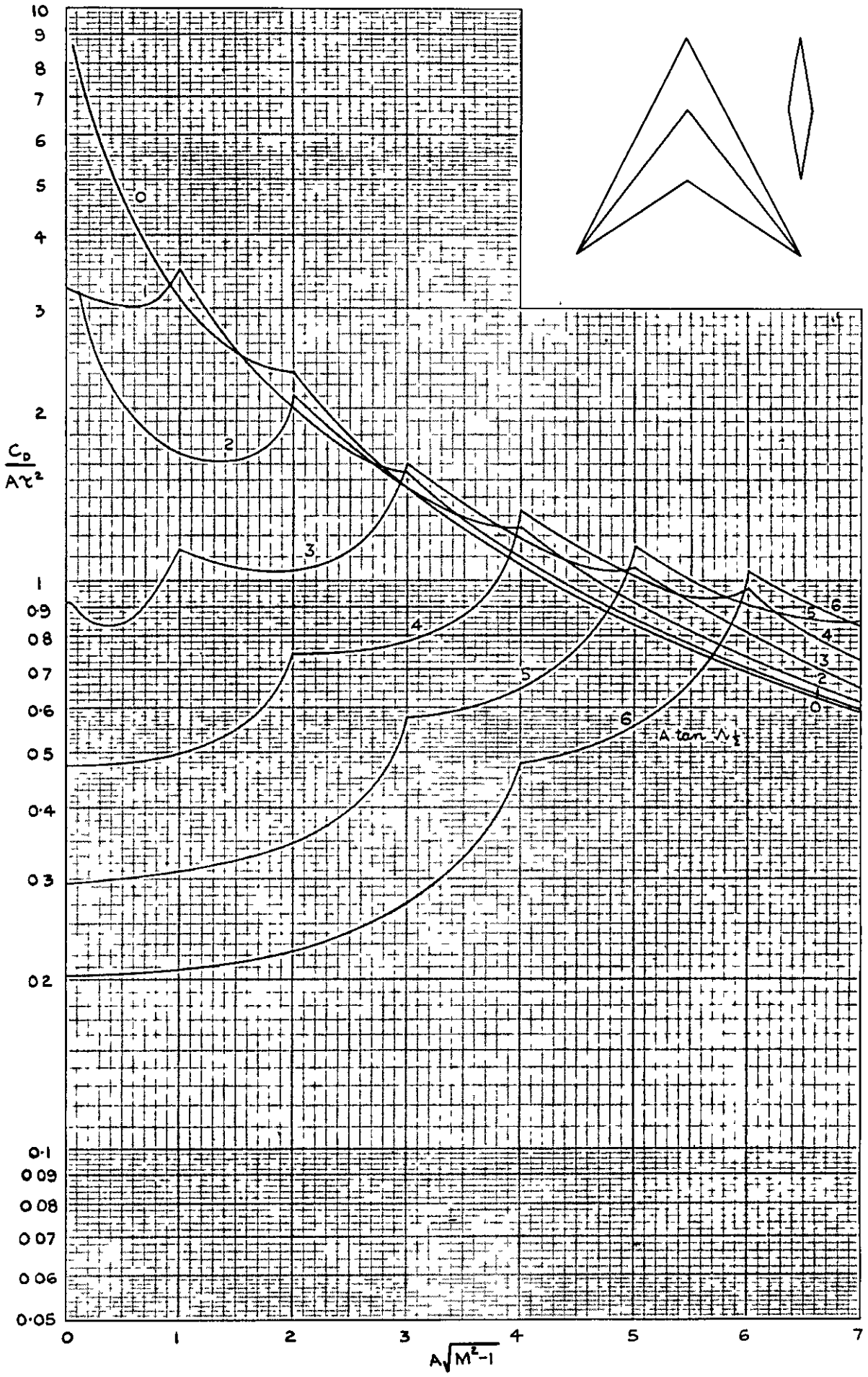

FIG 2 (d). WAVE DRAG OF WINGS OF DOUBLE-WEDGE SECTION.
$\lambda = 0$, $m = 0{\cdot}5$

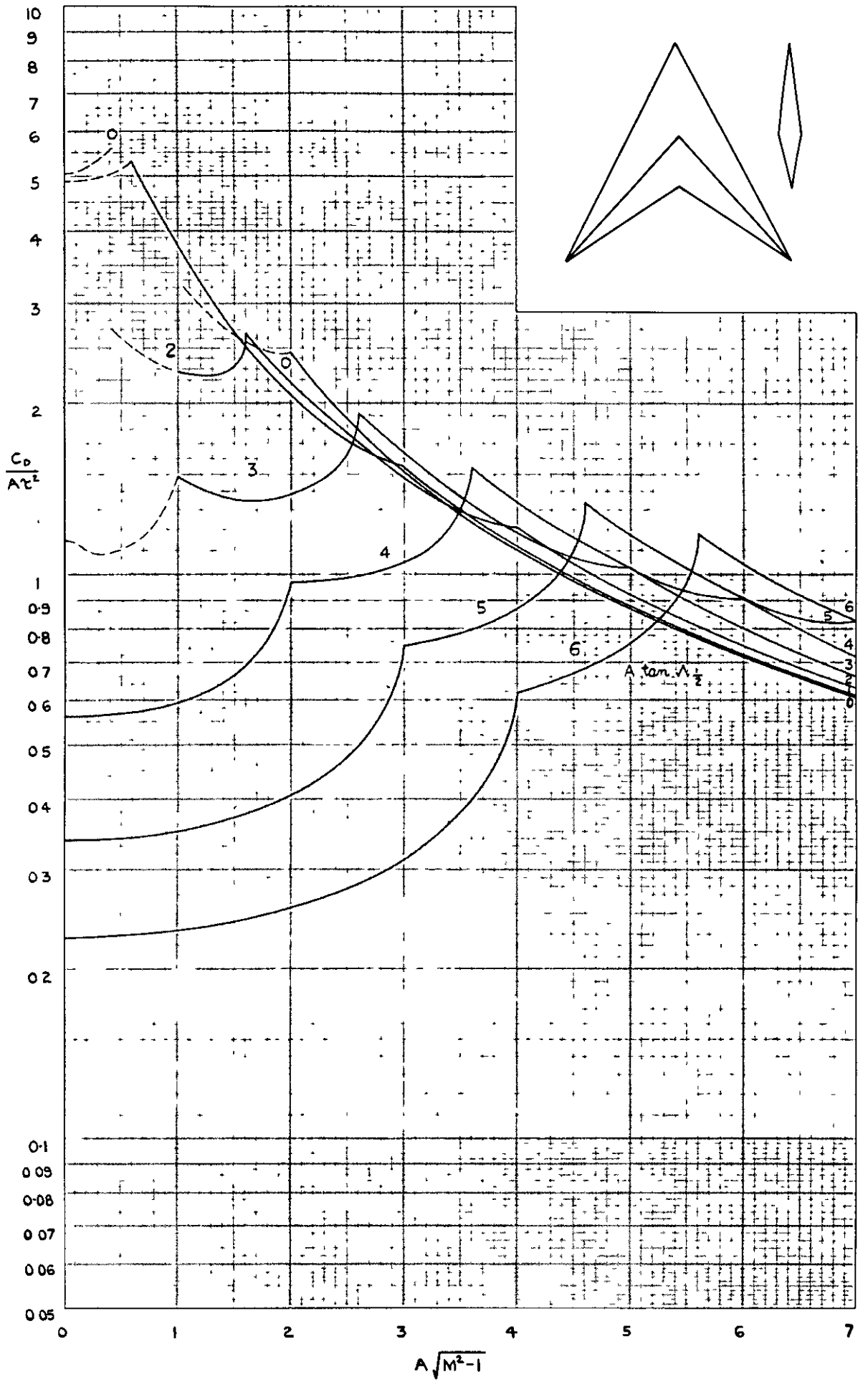

FIG. 2 (e). WAVE DRAG OF WINGS OF DOUBLE-WEDGE SECTION.

$\lambda = 0$, $m = 0{\cdot}6$

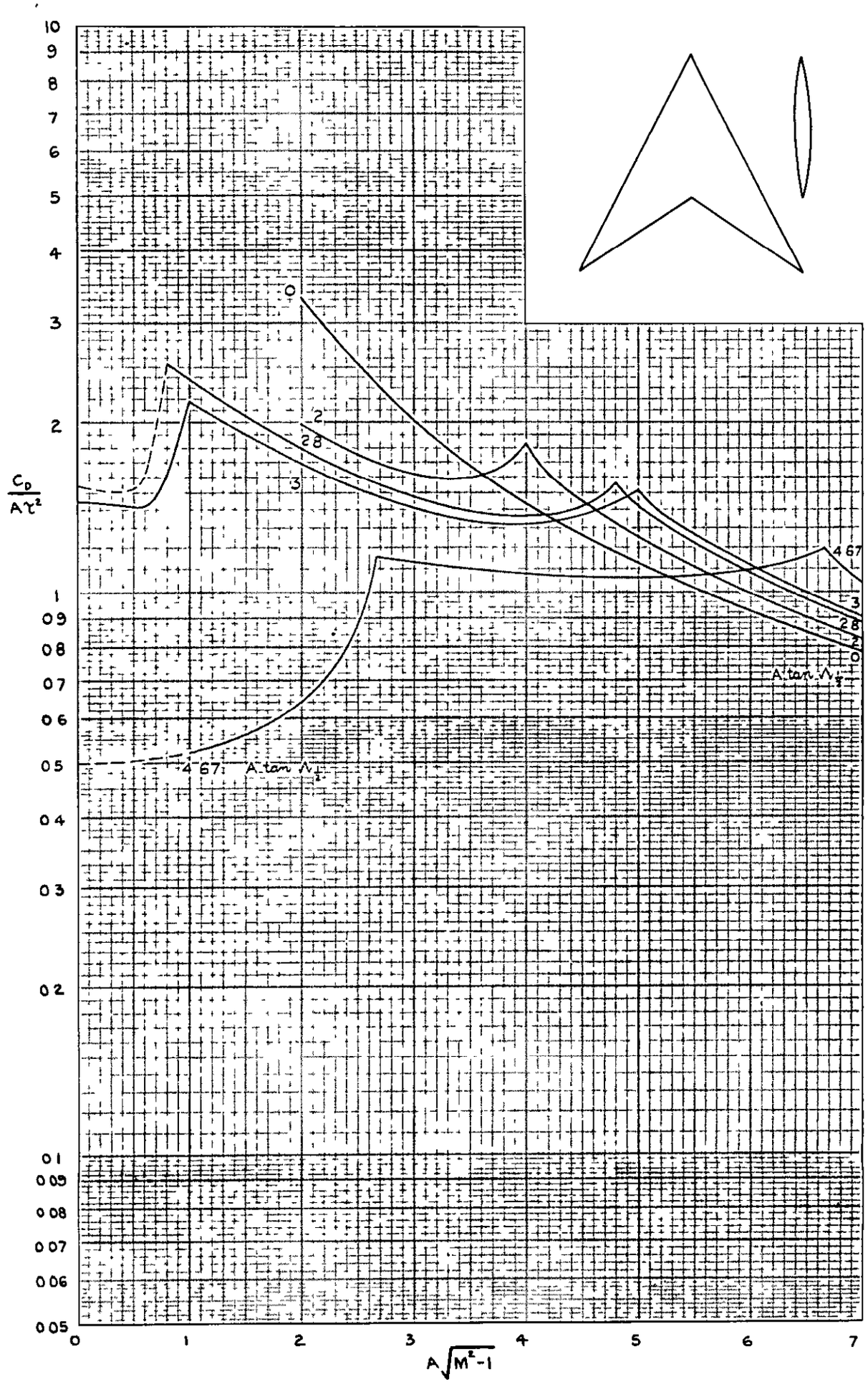

FIG. 2 (f). WAVE DRAG OF WINGS OF PARABOLIC-ARC SECTION.
$\lambda = 0$

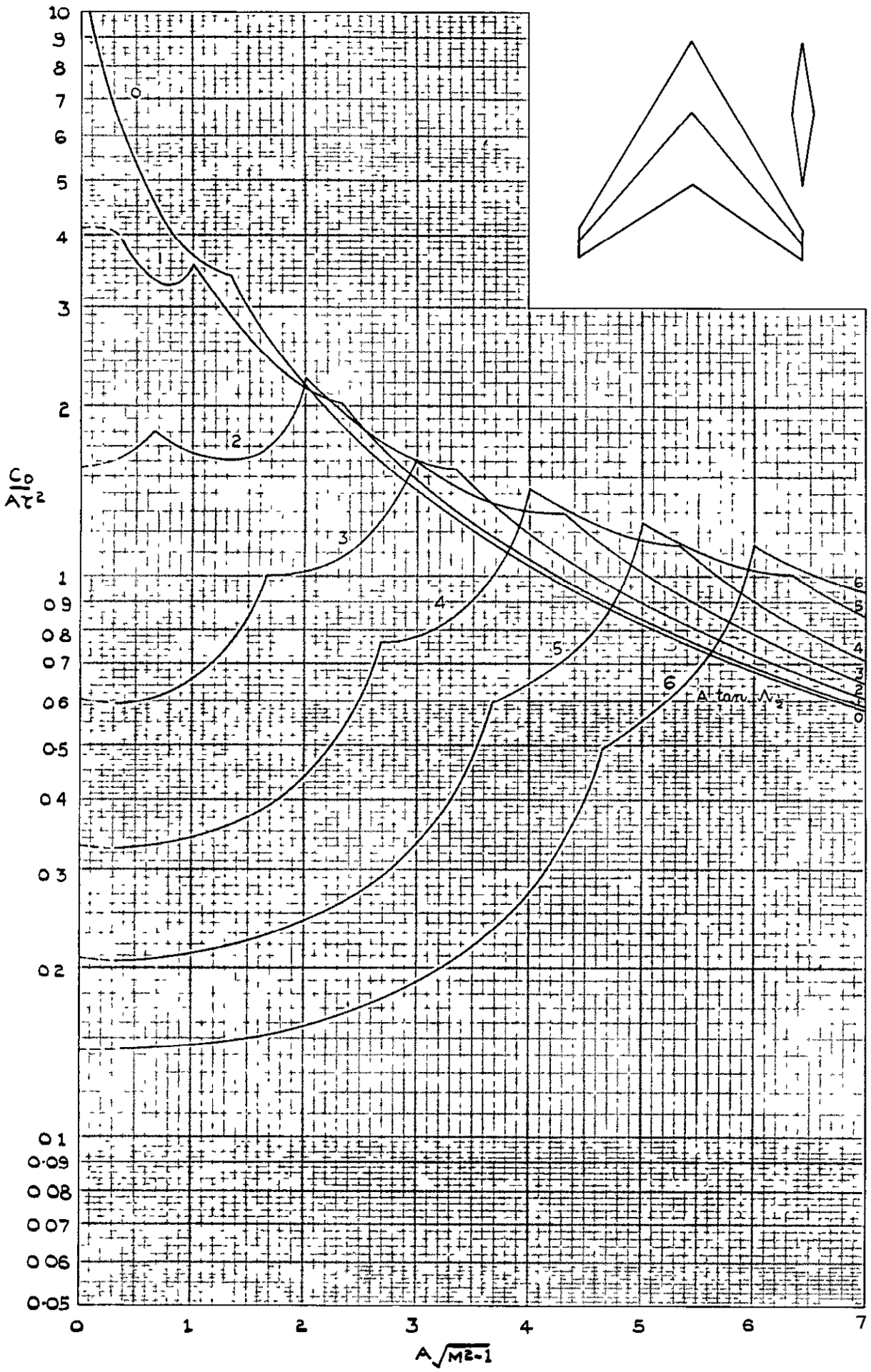

FIG. 3. WAVE DRAG OF WINGS OF DOUBLE-WEDGE SECTION

$\lambda = 0{\cdot}2.$ $m = 0{\cdot}5.$

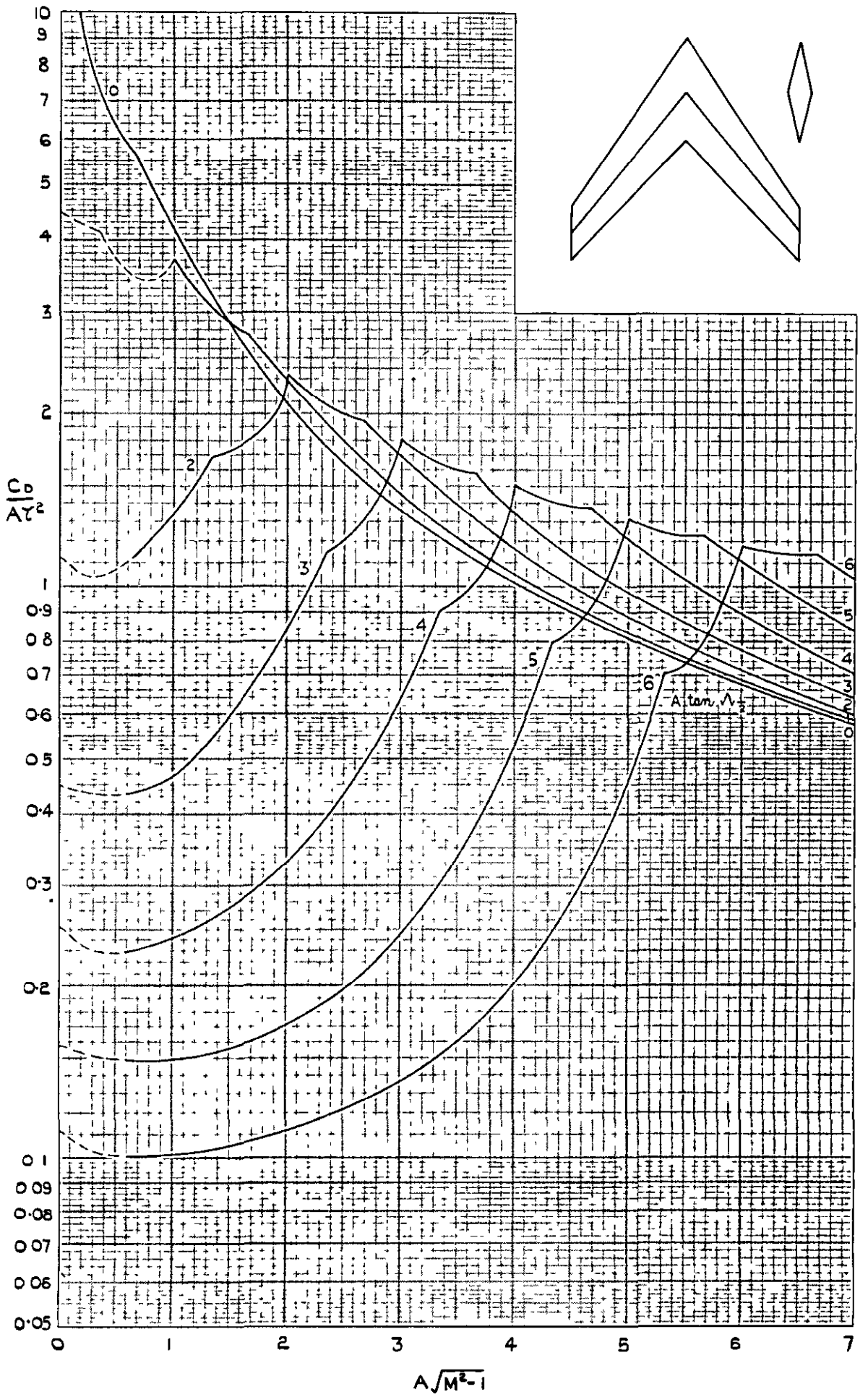

FIG. 4(a) WAVE DRAG OF WINGS OF DOUBLE-WEDGE SECTION.

$\lambda = 0.5$, $m = 0.5$.

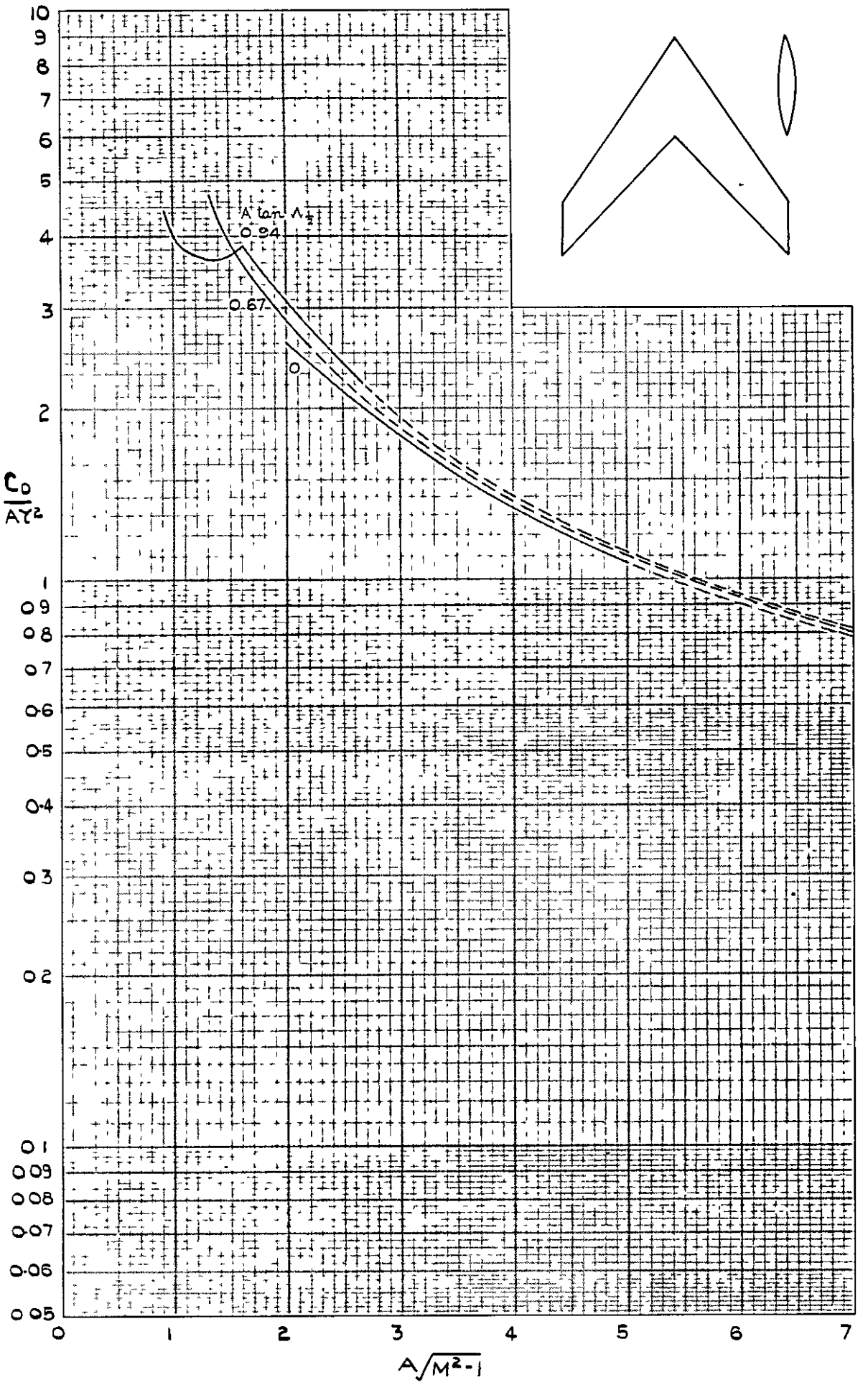

FIG. 4(b). WAVE DRAG OF WINGS OF PARABOLIC-ARC SECTION

$\lambda = 0.5$

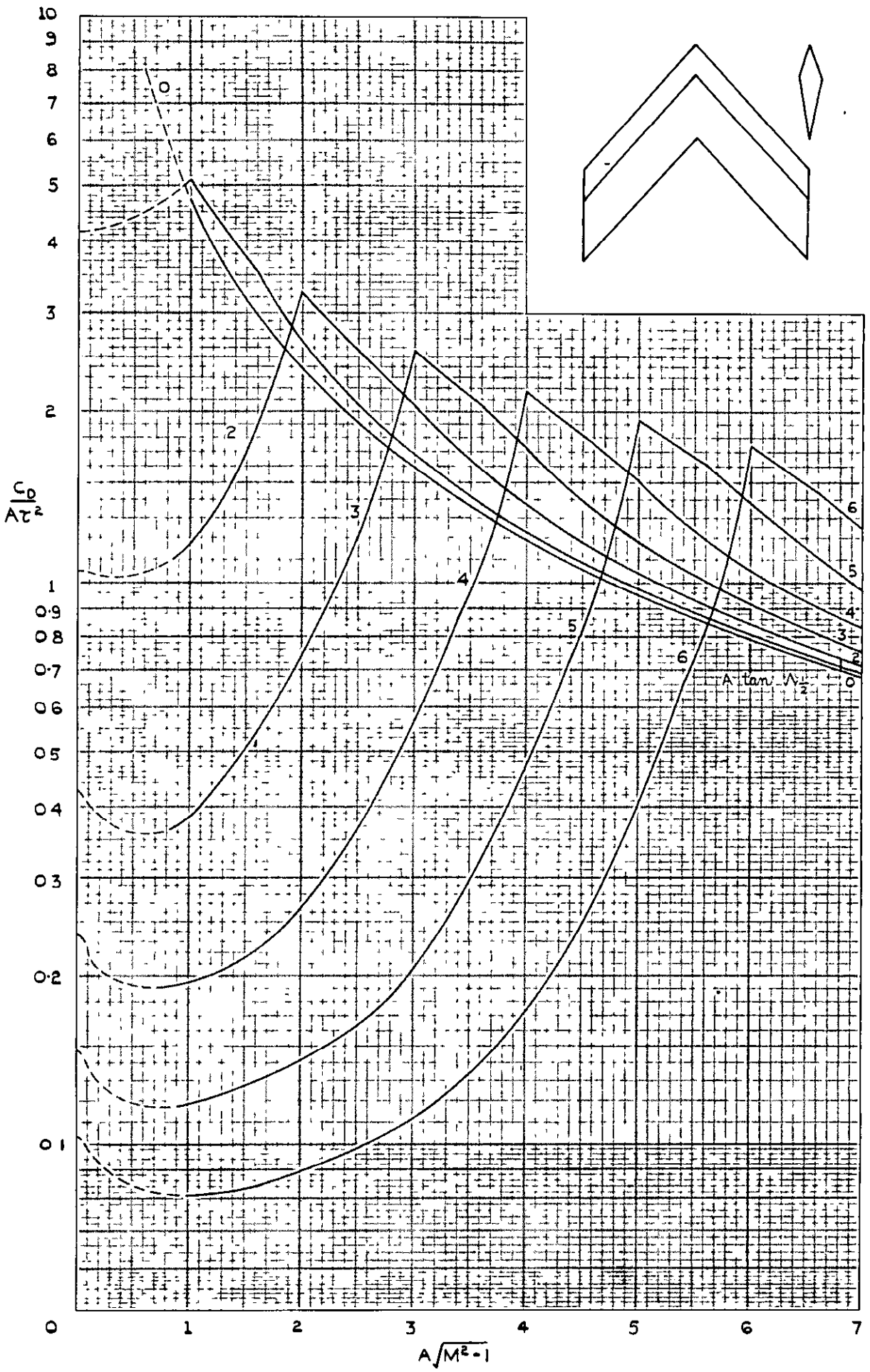

FIG. 5(a). WAVE DRAG OF WINGS OF DOUBLE-WEDGE SECTION.

$\lambda = 1$, $m = 0{\cdot}3$.

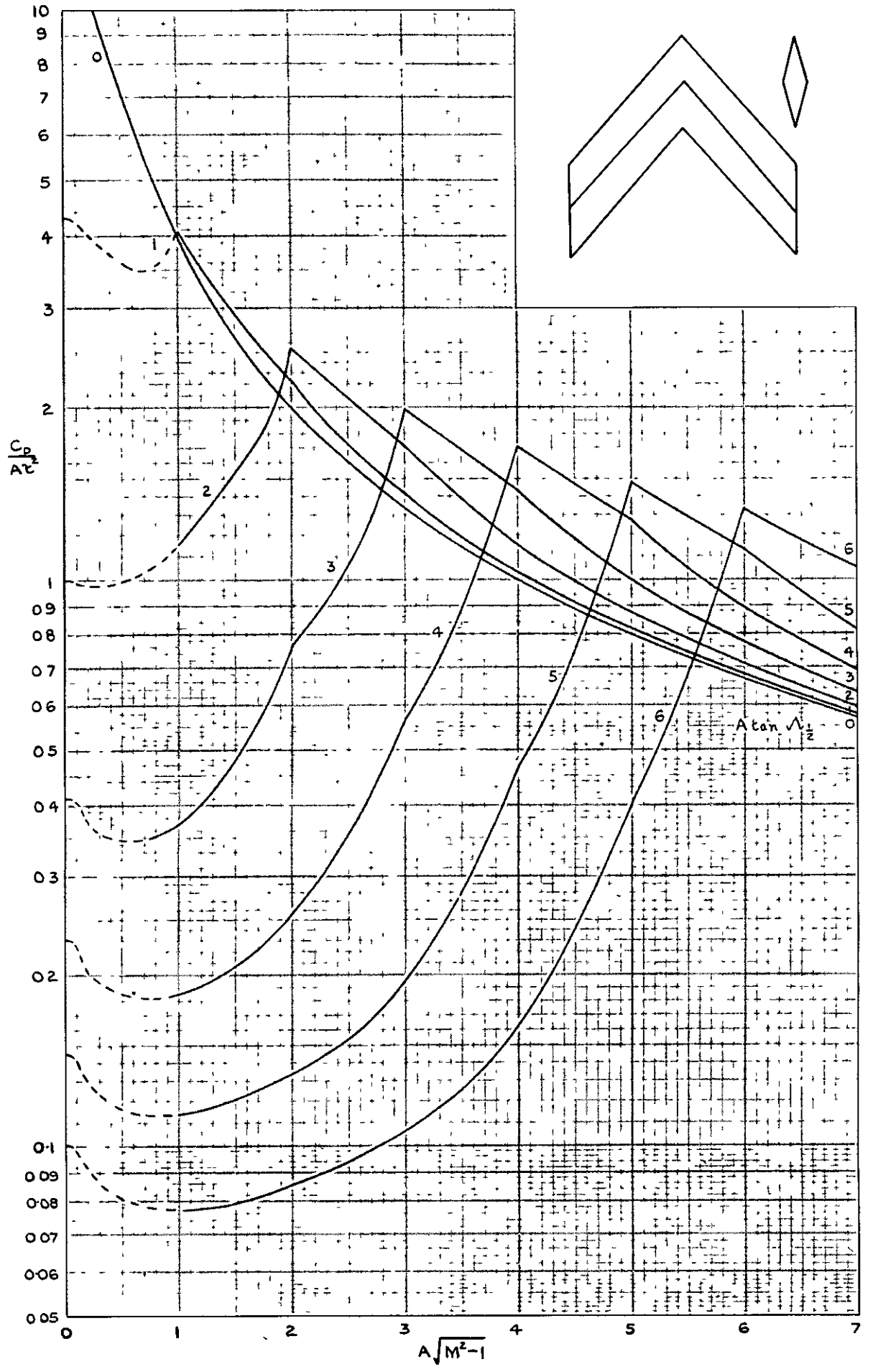

FIG. 5(b). WAVE DRAG OF WINGS OF DOUBLE-WEDGE SECTION.

$\lambda = 1$, $m = 0.5$

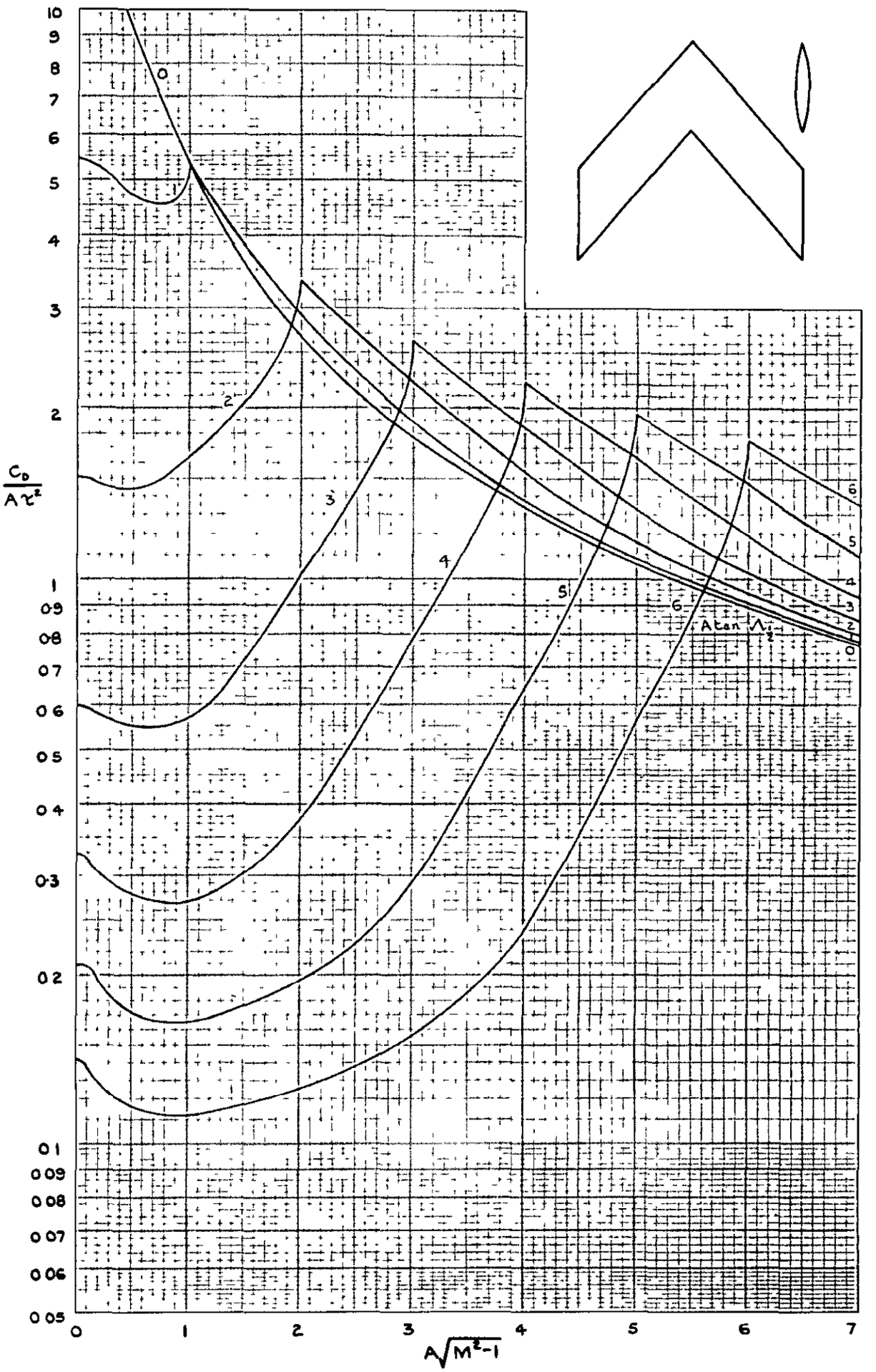

FIG.5 (c). WAVE DRAG OF WINGS OF PARABOLIC – ARC SECTION.

$\lambda = 1$

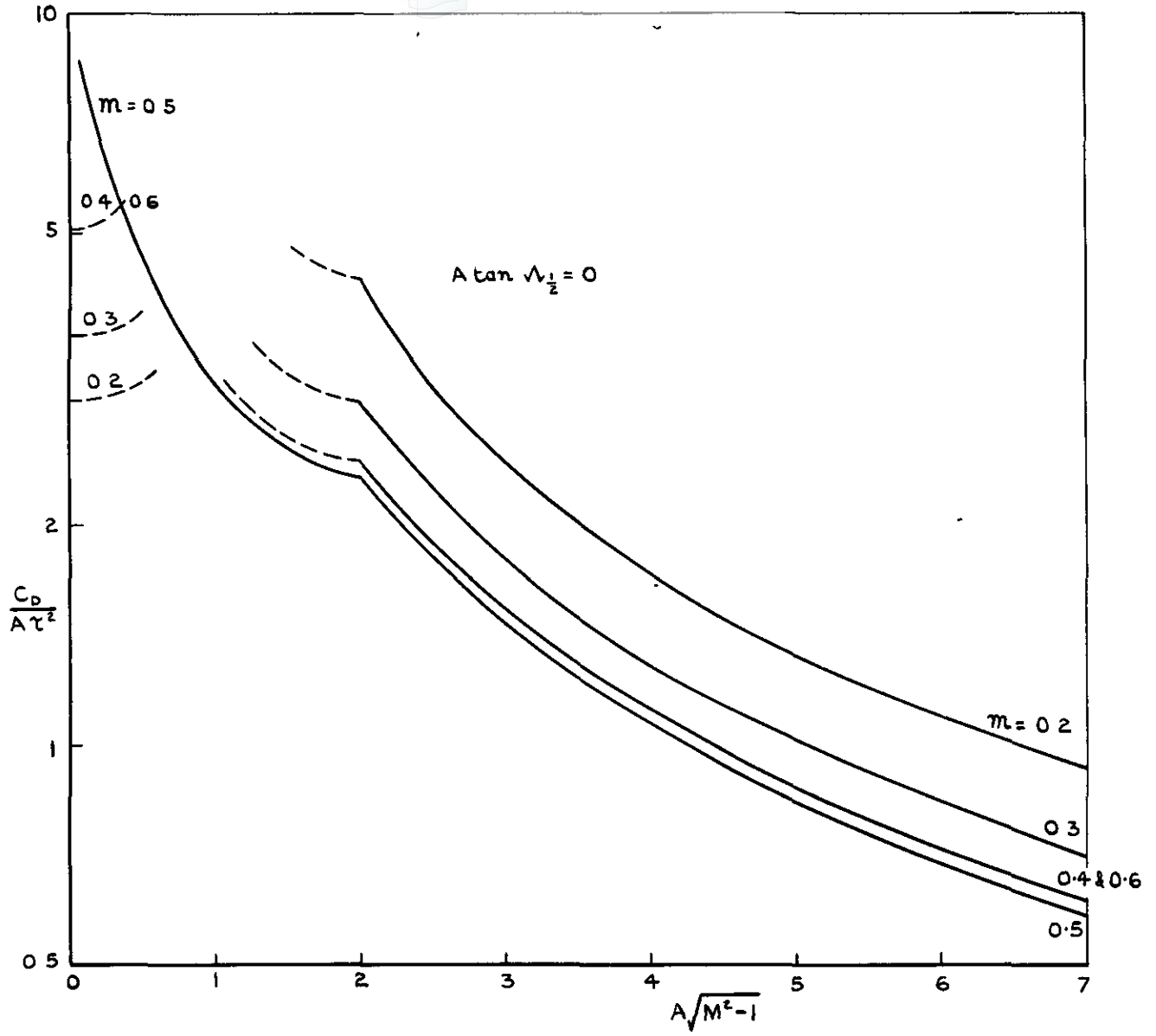

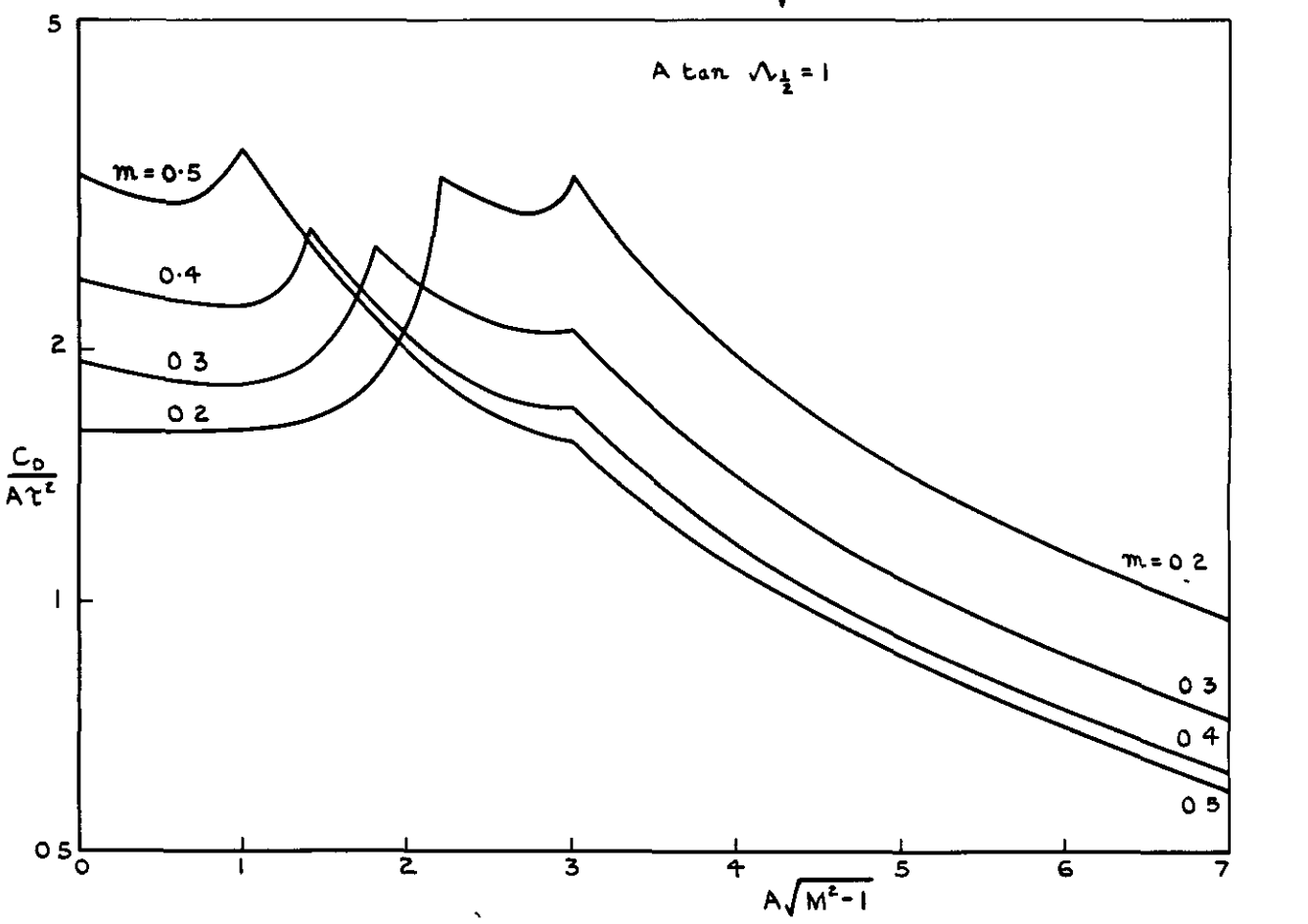

FIG. 6. EFFECT OF MAXIMUM THICKNESS POSITION ON THE WAVE DRAG OF WINGS OF DOUBLE WEDGE SECTION.
$\lambda = 0$

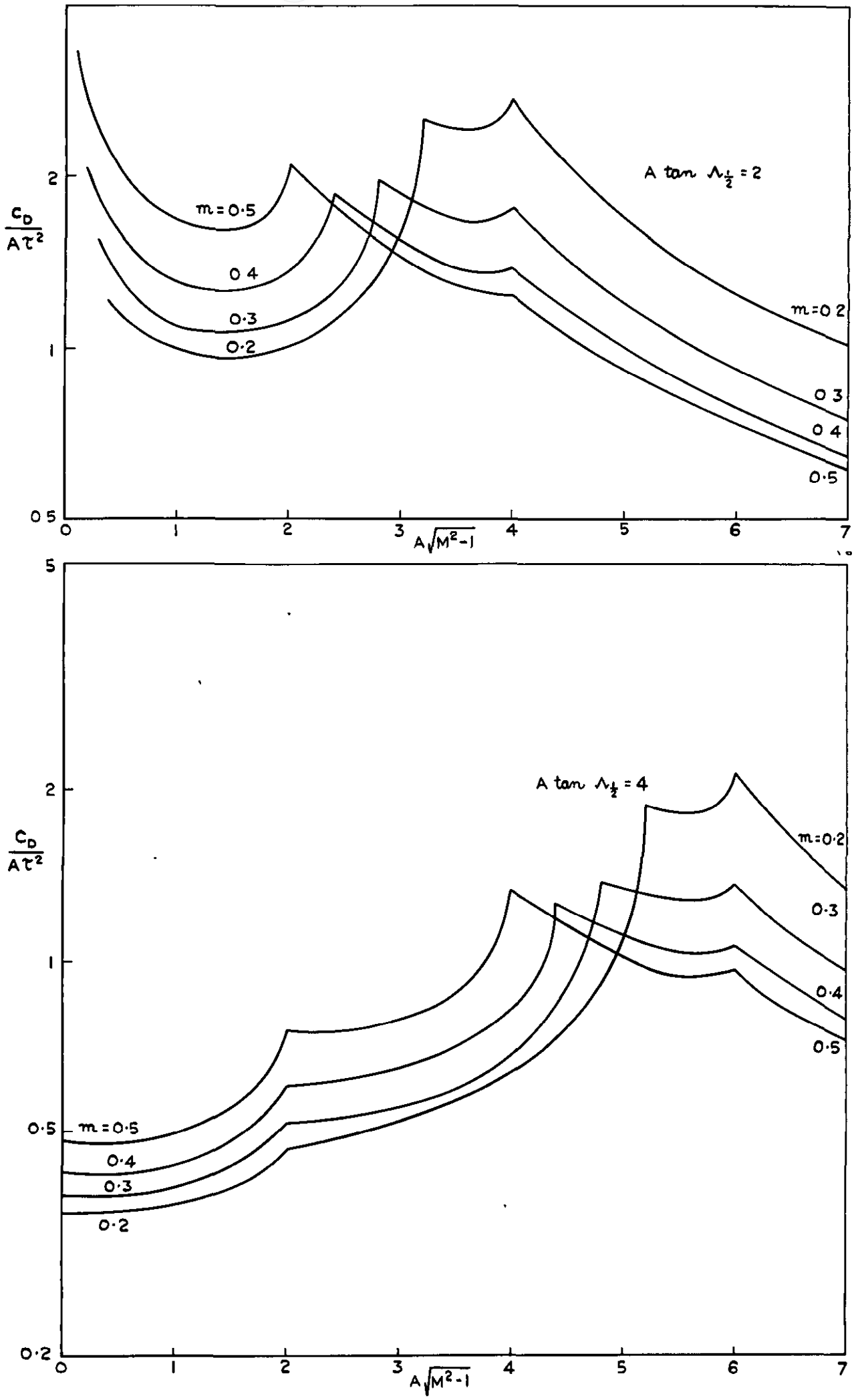

FIG. 6 (CONT'D). EFFECT OF MAXIMUM THICKNESS POSITION ON THE WAVE DRAG OF WINGS OF DOUBLE-WEDGE SECTION.
$\lambda = 0$.

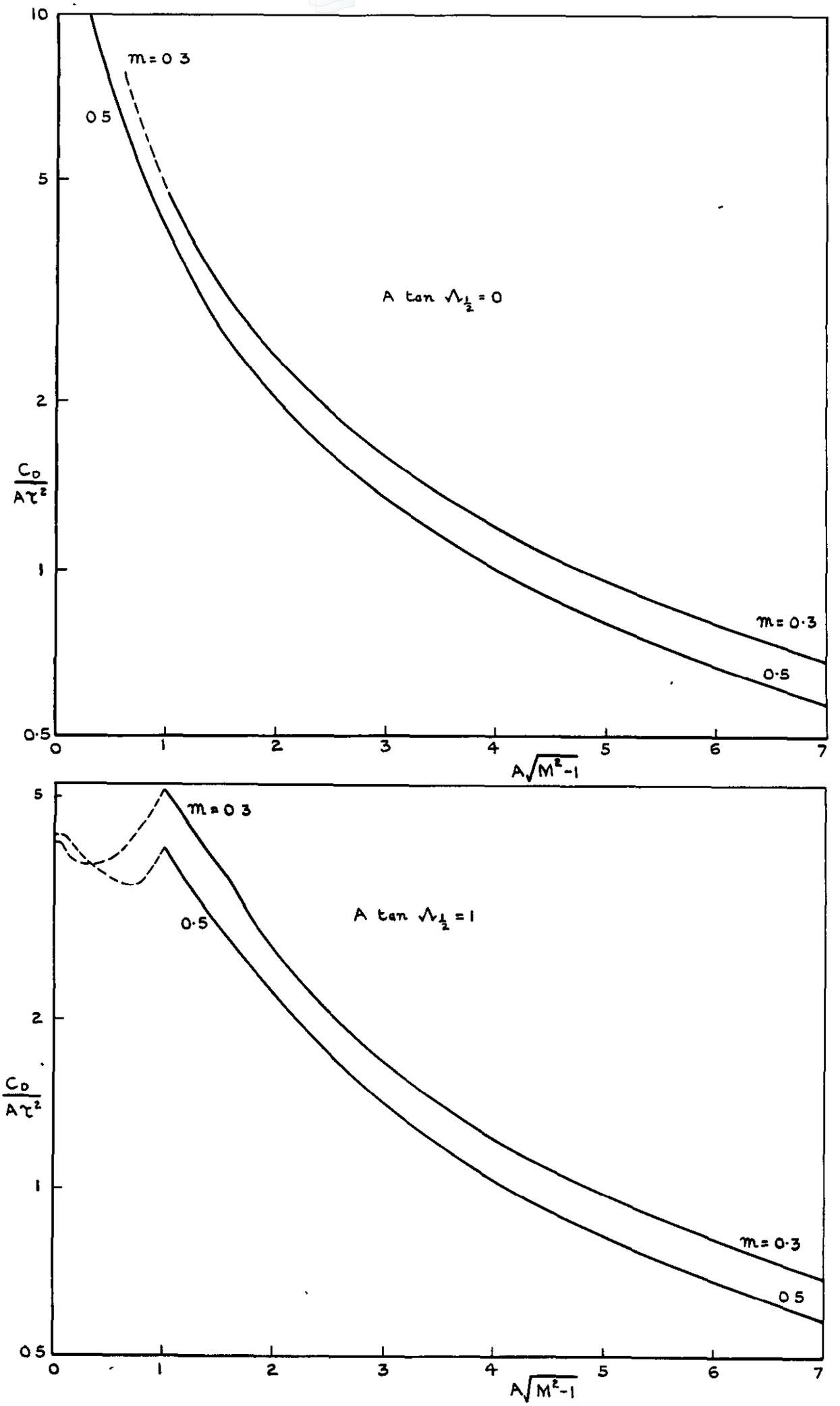

FIG. 7. EFFECT OF MAXIMUM THICKNESS POSITION ON THE WAVE DRAG OF WINGS OF DOUBLE WEDGE SECTION.
$\lambda = 1$

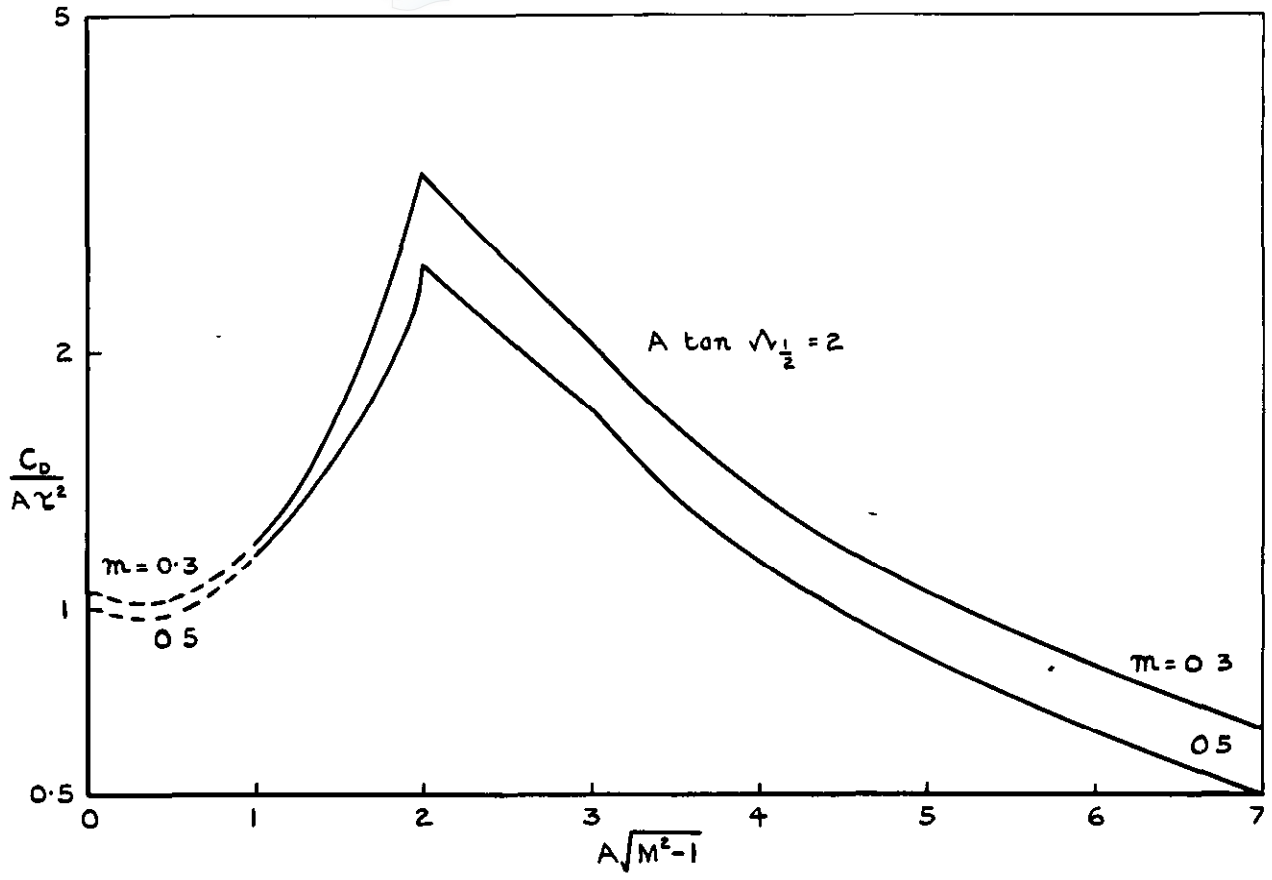

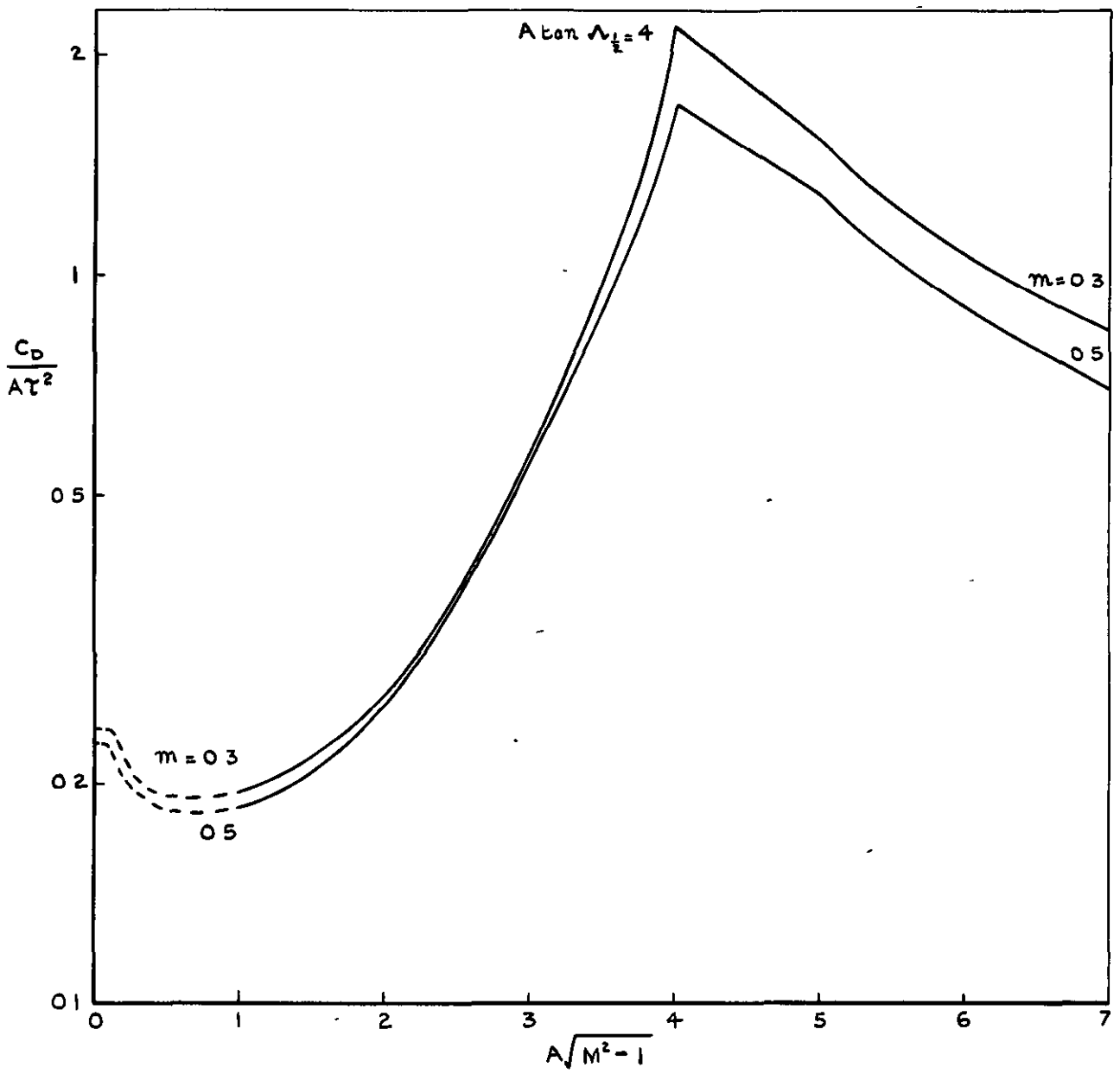

FIG. 7 (CONT'D). EFFECT OF MAXIMUM THICKNESS POSITION ON THE WAVE DRAG OF WINGS OF DOUBLE WEDGE SECTION.
$\lambda = 1$

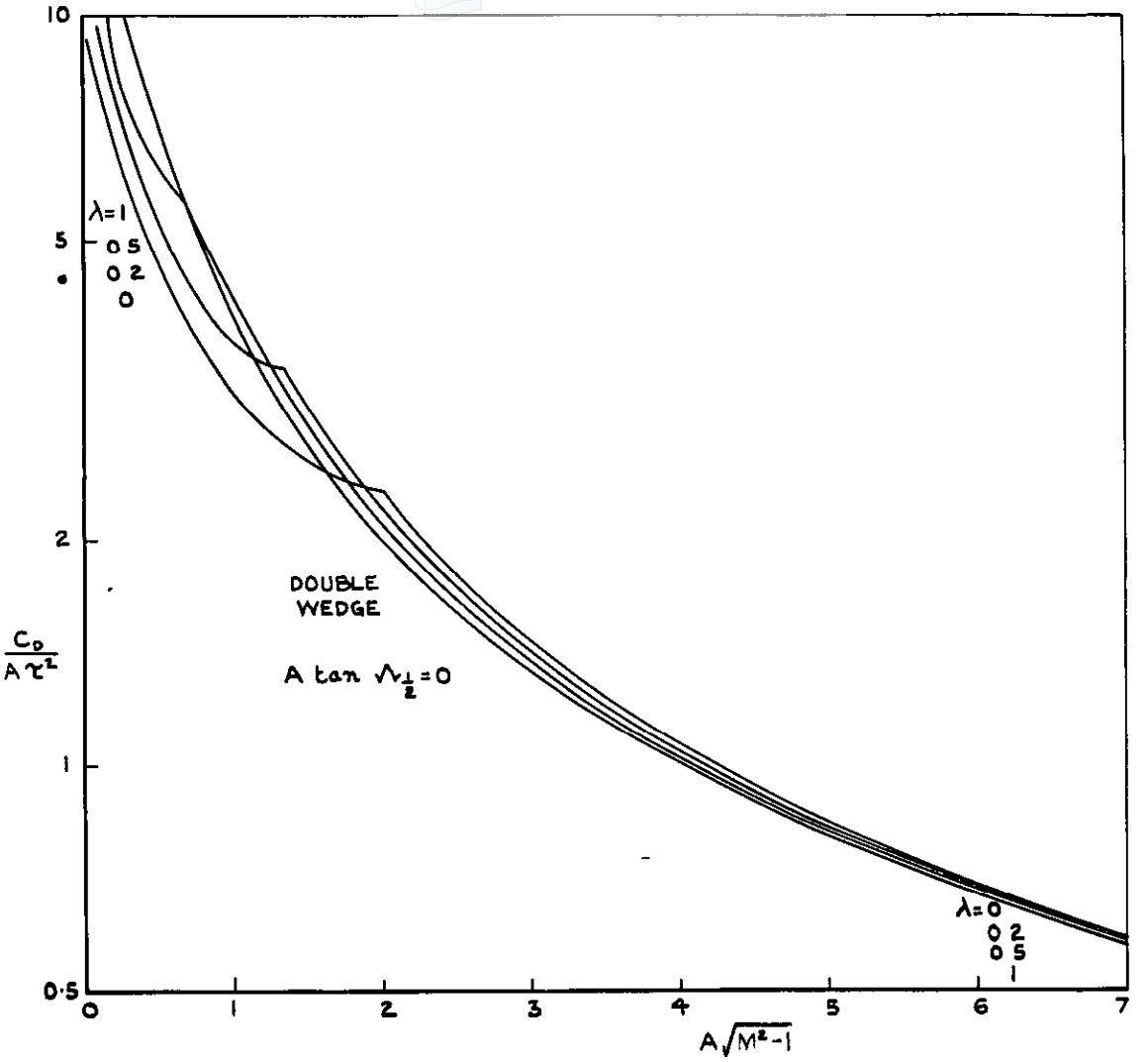

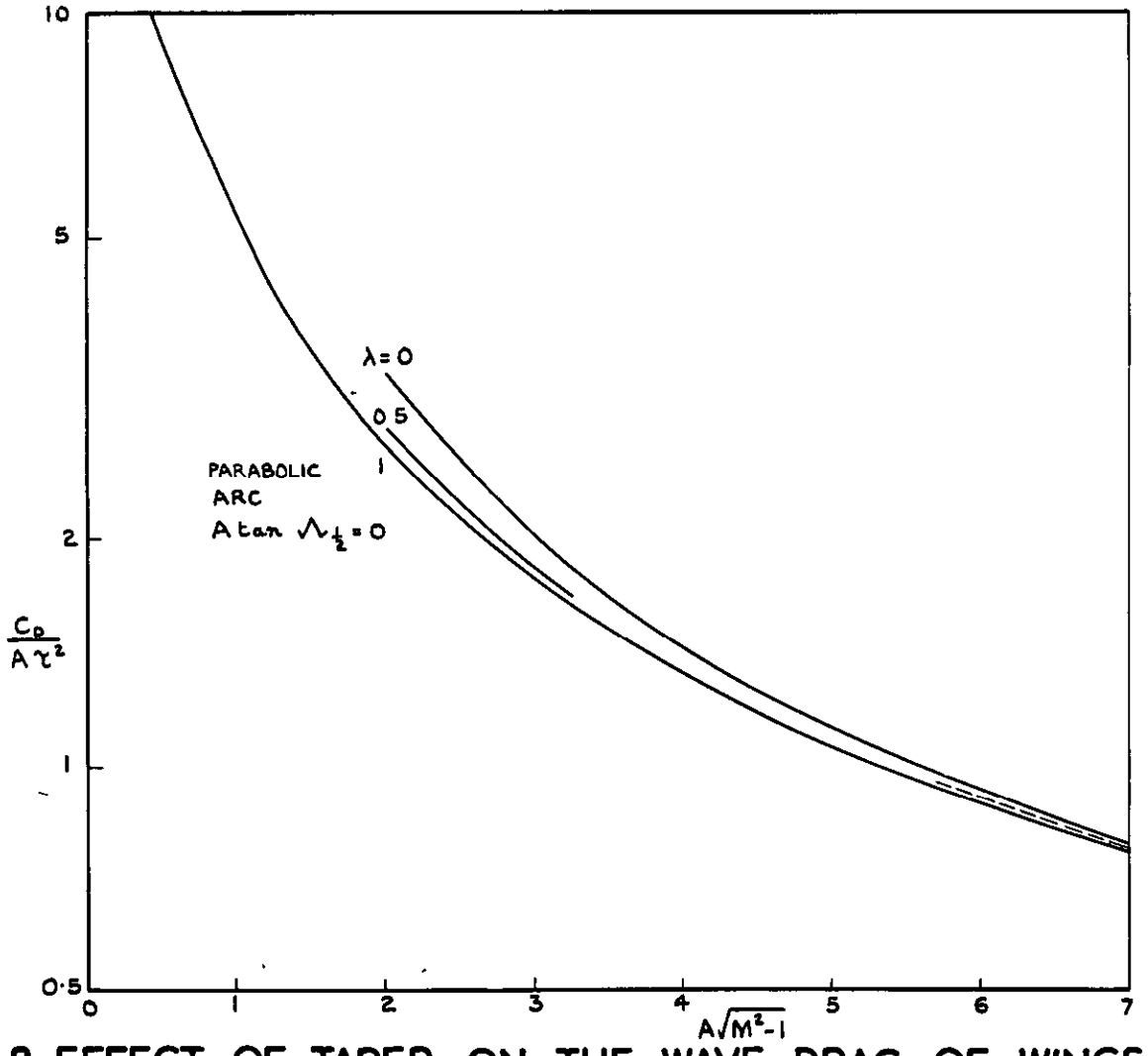

FIG.8. EFFECT OF TAPER ON THE WAVE DRAG OF WINGS OF DOUBLE WEDGE AND PARABOLIC ARC SECTIONS.
m = 0·5

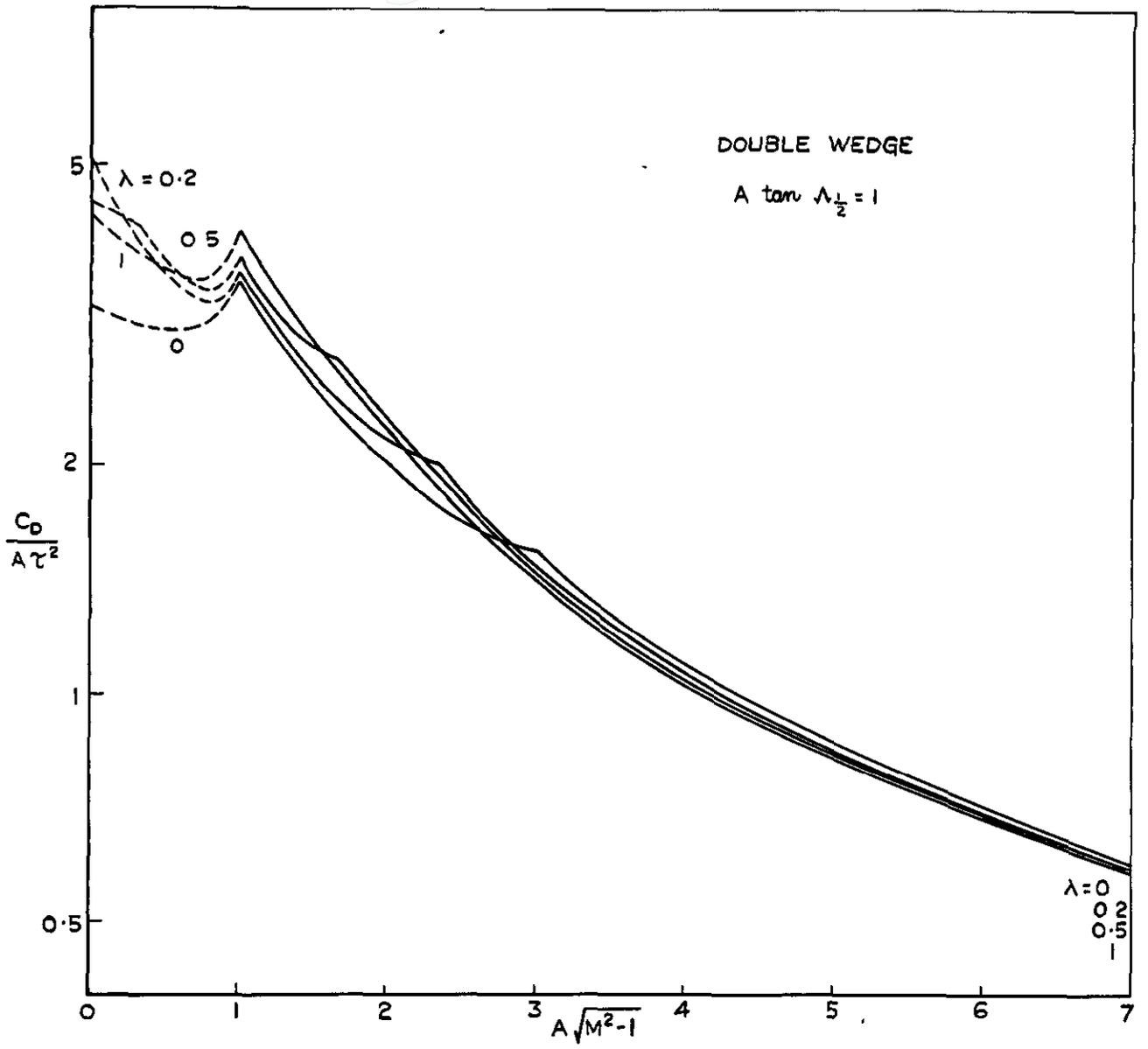

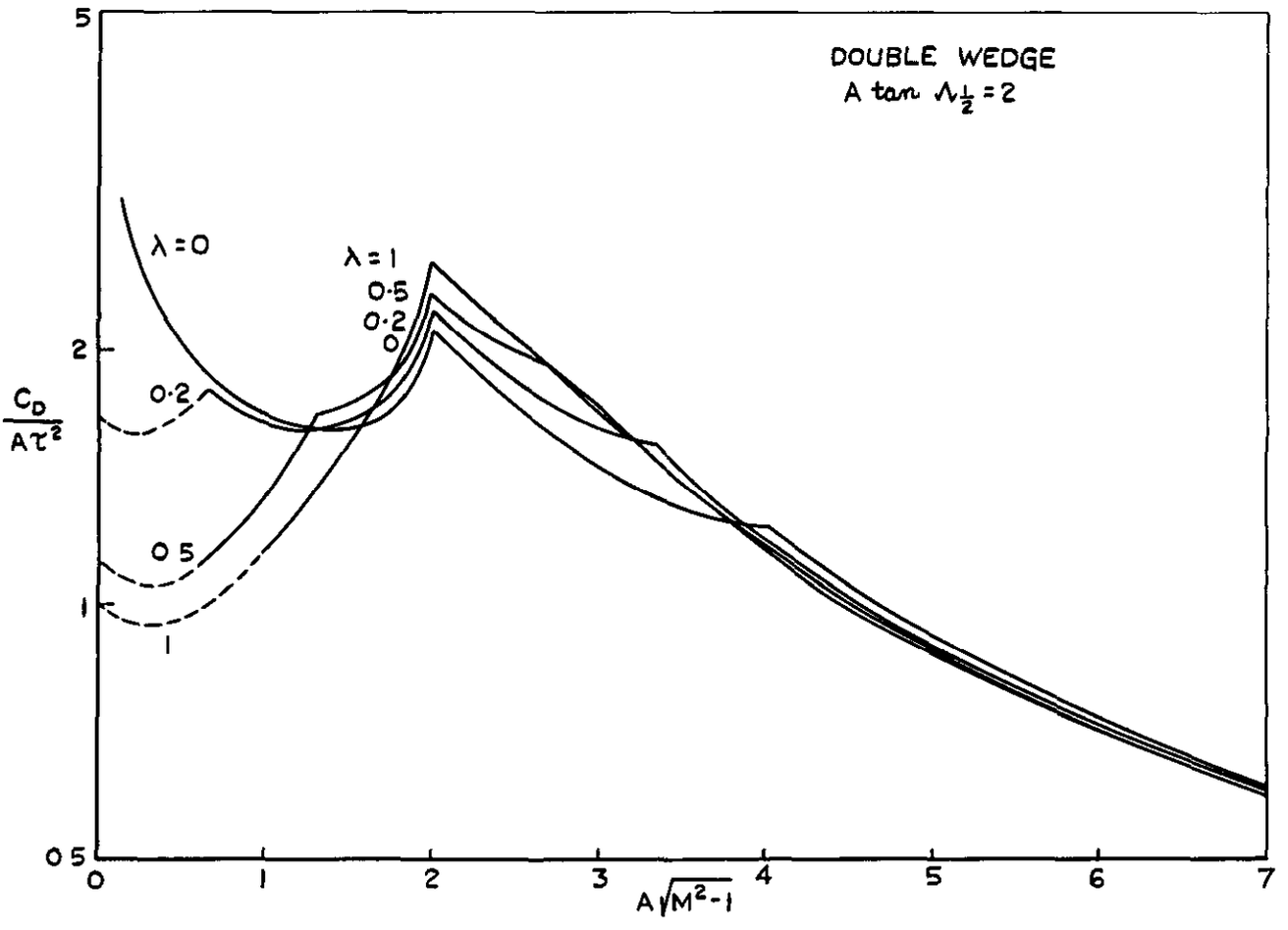

FIG.8 (CONT'D). EFFECT OF TAPER ON THE WAVE DRAG OF WINGS OF DOUBLE-WEDGE AND PARABOLIC-ARC SECTIONS.
m = 0·5.

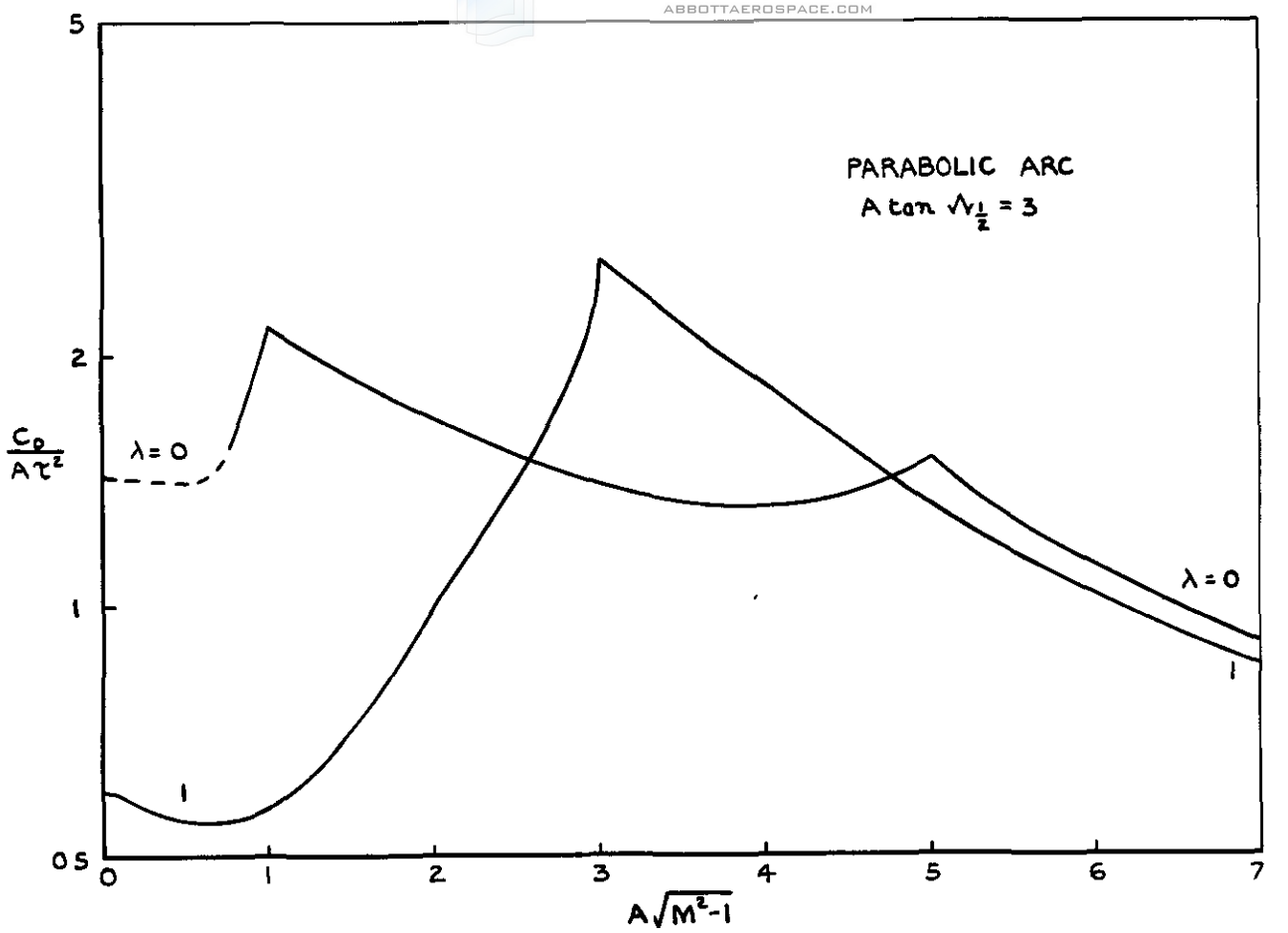

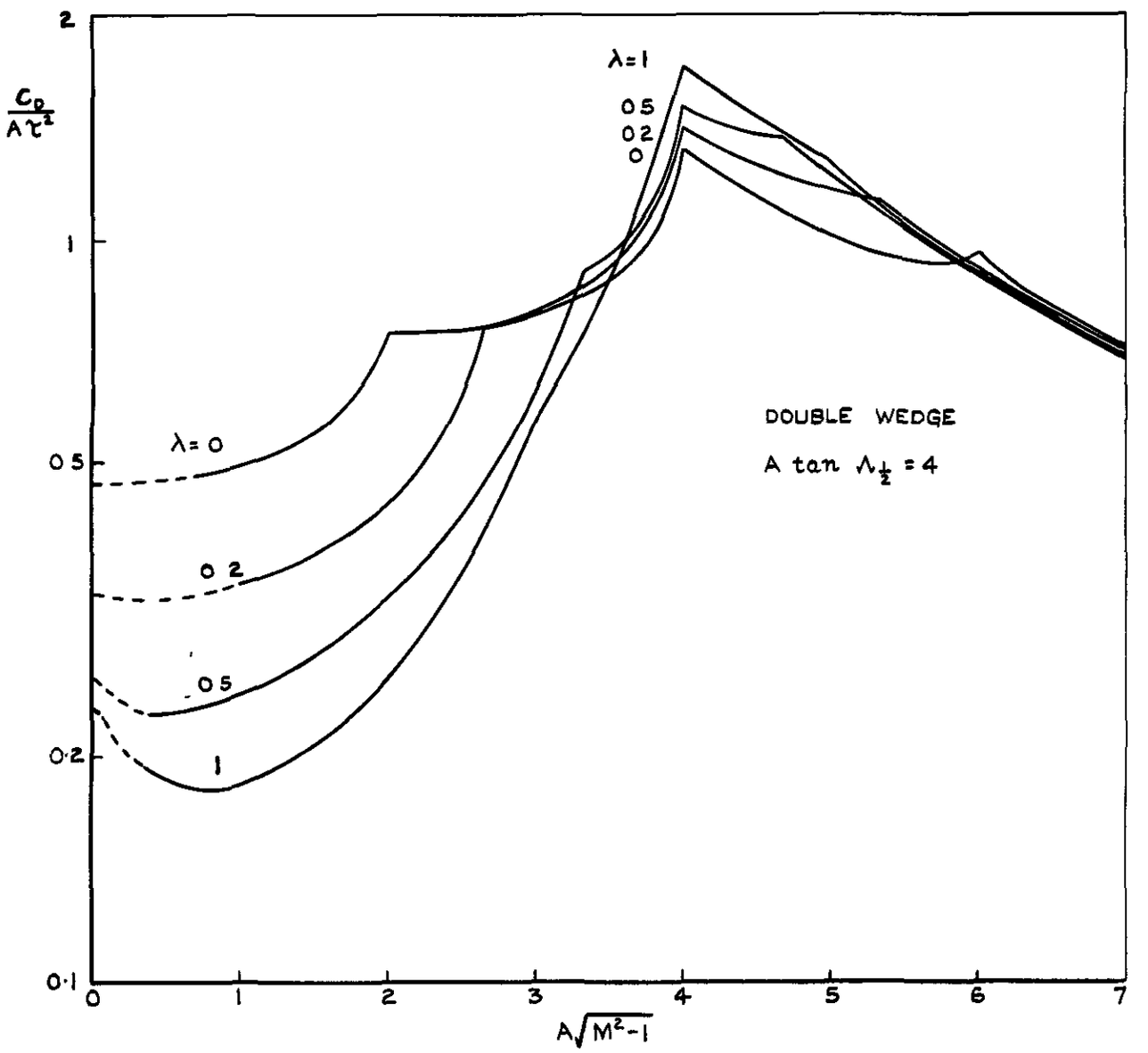

FIG.8 (CONT'D). EFFECT OF TAPER ON THE WAVE DRAG OF WINGS OF DOUBLE WEDGE AND PARABOLIC ARC SECTIONS.
m = 0·5

C.P. No. 313
(18,872)
A.R.C. Technical Report

Published by
HER MAJESTY'S STATIONERY OFFICE

To be purchased from
York House, Kingsway, London W C 2
423 Oxford Street, London W 1
P O Box 569, London S E 1
13A Castle Street, Edinburgh 2
109 St Mary Street, Cardiff
39 King Street, Manchester 2
Tower Lane, Bristol 1
2 Edmund Street, Birmingham 3
80 Chichester Street, Belfast
or through any bookseller

PRINTED IN GREAT BRITAIN

S.O. Code No. 23-9010-13

C.P. No. 313